Regional Holocene climate and landscape changes recorded in the large subarctic lake Torneträsk, N Fennoscandia

Carsten Meyer-Jacob[a,‡], Richard Bindler[a], Christian Bigler[a], Melanie J. Leng[b], Sally E. Lowick[c] and Hendrik Vogel[c]

[a] Department of Ecology and Environmental Science, Umeå University, 901 87 Umeå, Sweden; carsten.meyerjacob@gmail.com, richard.bindler@umu.se, christian.bigler@umu.se

[b] NERC Isotope Geosciences Facilities, British Geological Survey, Nottingham, NG12 5GG, UK & Centre for Environmental Geochemistry, University of Nottingham, Nottingham, NG7 2RD, UK, mjl@bgs.ac.uk

[c] Institute of Geological Sciences and Oeschger Centre for Climate Change Research, University of Bern, Baltzerstrasse 1+3, 3012 Bern, Switzerland, lowick@geo.unibe.ch, hendrik.vogel@geo.unibe.ch

[‡] Corresponding author (Email: carsten.meyerjacob@gmail.com)

Abstract

Understanding the response of sensitive Arctic and subarctic landscapes to climate change is essential to determine the risks of ongoing and projected climate warming. However, these responses will not be uniform in terms of timing and magnitude across the landscape because of site-specific differences in ecosystem susceptibility to climate forcing. Here we present a multi-proxy analysis of a sediment record from the 330-km^2 lake Torneträsk to assess the sensitivity of the Fennoscandian subarctic landscape to climate change over the past ~9500 years. By comparing responses of this large-lake system to past climatic and environmental changes with those in small lakes in its catchment, we assessed when the magnitude of change was sufficient to affect an entire region rather than only specific sub-catchments that may be more sensitive to localized environmental changes such as, e.g., tree-line dynamics. Our results show three periods of regional landscape alteration with distinct change in sediment composition: i) landscape development following deglaciation and through the Holocene Thermal Maximum, ~9500-3400 cal yr BP; ii) increased soil erosion during the Little Ice Age (LIA); and iii) rapid change during the past century coincident with ongoing climate change. The gradual landscape development led to successive changes in the lake sediment composition over several millennia, whereas climate cooling during the late Holocene caused a rather abrupt shift occurring within ~100 years. However, this shift at the onset of the LIA (~750 cal yr BP) occurred >2000 years later than the first indications for climate cooling recorded in small lakes in the Torneträsk catchment, suggesting that a critical ecosystem threshold was not crossed until the LIA. In contrast, the ongoing response to recent climate change was immediate, emphasizing the unprecedented scale of ongoing climate changes in subarctic Fennoscandia.

Keywords: Inorganic geochemistry; Soil erosion; Climate change; Oxygen and silicon isotopes; Holocene; Scandinavia.

1. Introduction

Landscapes in the Arctic and subarctic are undergoing extensive transformations because of ongoing climate change. In these landscapes, climate change leads to pronounced changes in land cover and vegetation composition (e.g., Zhang et al., 2013) as well as to the degradation of permafrost, which alters hydrology and slope stability (e.g., Hinzman et al., 2005). These dynamics in turn cause climate feedbacks, particularly by affecting carbon cycling and release of greenhouse gases (Pearson et al., 2013; Schuur et al., 2015). However, the scale of this transformation is not uniform across northern landscapes (e.g., Elmendorf et al., 2012; Xu et al., 2013).

Lakes can respond rapidly to changes in climate forcing with regard to their physical (e.g., water temperature, thermal stratification, ice cover duration), chemical (e.g., oxygen levels, carbon and nutrient cycling), and biological (e.g., phenology, food web structure) characteristics (Williamson et al., 2009). In addition to immediate in-lake responses, there are also responses in the aquatic and surrounding terrestrial systems that occur over centuries to millennia. Lakes integrate information on these long-term changes and may archive them in their sediments. Responses to long-term changes, such as variations in vegetation cover, soil development or catchment erosion, are non-linear because of complex forcing-response relationships. Furthermore, lakes may show variable responses to climate changes because of differences in characteristics; for example, small, shallow lakes with a low heat capacity may respond rapidly to small changes and thus

present higher-frequency noise in limnological and paleolimnological data (Adrian et al., 2009). With increased lake and watershed size, initial small-scale changes in the watershed are recorded at different scales in these cascading systems and potentially with time lags (cf., Dearing and Jones, 2003). This lower sensitivity of larger drainage basins to local changes allows the determination of the timing and character of important environmental tipping points, i.e., changes that are of sufficient magnitude to affect an entire region rather than only specific areas of a watershed that are particularly sensitive to climate/environmental changes, e.g., tree-line lakes.

In northernmost Sweden in the subarctic catchment of the large lake Torneträsk ("Torne Lake" in English; surface area: 330 km^2; watershed: 3350 km^2; Fig. 1), the observed climate change during the past century has thus far led to a mean annual temperature increase of 2.5°C, a shortened (~40 days) lake ice cover period (Callaghan et al., 2013), a reduced permafrost thickness (Åkerman and Johansson, 2008), and an increase of wet areas in mires due to permafrost degradation (Malmer et al., 2005). The Torneträsk area has been subject to numerous studies in different disciplines focusing on a modern process understanding, including carbon cycling (e.g., Christensen et al., 2007; Karlsson et al., 2010), permafrost dynamics (e.g., Åkerman and Johansson, 2008; Kokfelt et al., 2009), and sediment transport (e.g., Beylich et al., 2006). In addition to these studies on recent processes, sediment records from several small lakes in the catchment have been studied to reconstruct Holocene climate and environmental change with a focus on vegetation development (e.g., Barnekow, 1999; 2000), quantitative climate reconstructions (e.g., Bigler et al., 2002; 2003), sediment transport and erosion (e.g., Snowball and Sandgren, 1996; Rubensdotter and Rosqvist, 2003) and changes in atmospheric circulation patterns (e.g., Hammarlund et al., 2002; Rosqvist et al., 2007; Shemesh et al., 2001) (Fig. 1).

Because of the complexity and multitude of studies of small lakes conducted in the Torneträsk catchment, a study of the lake itself represents an ideal site for investigating the integrated regional climatic and environmental development in northernmost Sweden since the retreat of the Fennoscandian ice sheet. Studies of Torneträsk's sediment record are thus far scarce and have only focused on a general sedimentological description of the lacustrine sediment (Andrén et al., 2002), recent changes in the input of terrestrial organic matter (OM) (Vonk et al., 2012) and on depositional patterns and subaquatic topography (Vogel et al., 2013).

Using a combination of geochemical, isotopic and biological proxies, the aims of this multi-proxy study are twofold. One aim was to survey the surface sediment geochemistry in order to assess spatial variability, how this variability relates to catchment influences, and how signals might vary across this 70-km-long lake. The second and main aim was to analyze a complete sediment sequence from Torneträsk in order to determine the regional climate and environmental development in northernmost Sweden during the Holocene and to assess i) how responses to environmental change are recorded in the large lake system compared to small lakes that have been studied within its catchment, and ii) to what extent the ongoing climate change has already affected the lake ecosystem, and how the scale of any identified changes compares to changes that occurred during past periods of distinct climate change such as the Holocene Thermal Maximum (HTM) or the Little Ice Age (LIA).

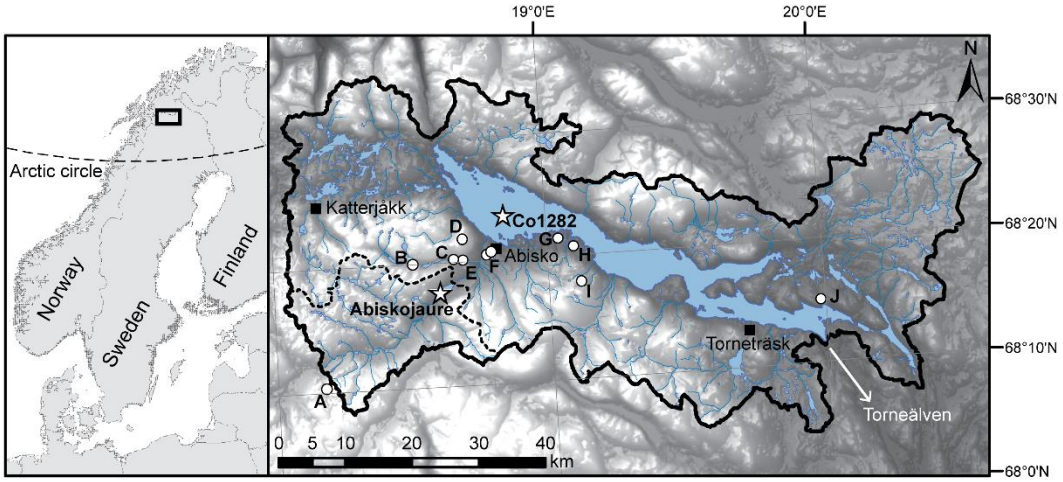

Figure 1. (left) Map over Fennoscandia showing the location of the study region. (right) Elevation map over the watershed of Torneträsk (black contour line). Dashed contour line defines the watershed of Abiskojaure, filled squares indicate the location of three weather stations (Swedish Meteorological and Hydrological Institute) across the Torneträsk catchment, while open stars mark the sampling sites in Torneträsk (core Co1282) and Abiskojaure. Open circles indicate locations of paleolimnological studies on smaller lakes from the area (A: Vuolep Allakasjaure, B: Kårsa valley lakes, C: Pikkujärvi, D: Lake Njulla, E: Lake Tibetanus, F: Vuolep Njakajaure and Badsjön, G: Villasjön and Inre Harrsjön, H: Vuoskkujávri, I: Lake 850/865, J: Lake Latteluokta. The white arrow highlights the outlet of Torneträsk, Torneälven, in the SE.

2. Regional setting

Torneträsk (68° 29'-68° 11' N, 20° 01'-18° 36' E; 341 m a.s.l.) is 70 km long (NW-SE), maximally 10 km wide (SW-NE), has a surface area of 330 km^2 and a watershed of 3350 km^2 (Fig. 1). The lake has an average depth of 53 m and a maximum depth of 168 m (based on bathymetric measurements in 1920/1921, Abisko Research Station; Fig. 2), with an estimated

115 water residence time of c. 8.5 years (Swedish Meteorological and Hydrological Institute (SMHI);
116 https://vattenwebb.smhi.se/). The watershed is drained by several smaller streams and rivers of
117 which the Abiskojåkka, entering the lake west of the village of Abisko, is the largest inlet with an
118 average discharge of 14 $m^3 \cdot s^{-1}$ (Fig. 1). Torneälven ("Torne River" in English) drains Torneträsk
119 to the SE with an average discharge of 65 $m^3 \cdot s^{-1}$ (1999–2013; SMHI; https://vattenwebb.smhi.se/)
120 (Fig. 1). The lake is (ultra)oligotrophic (TN = 195±25 $\mu g \cdot l^{-1}$, TP = 3±2 $\mu g \cdot l^{-1}$, TOC = 1.3±0.5
121 $mg \cdot l^{-1}$), circumneutral (pH = 7.3±0.1) (environmental monitoring data (MVM);
122 http://www.slu.se/miljodata-MVM), and $\delta^{18}O$ and $\delta^{2}H$ of water samples from Torneträsk were –
123 12.7/–12.8‰ and –92.6/–93.0‰, respectively in August 1999 (Shemesh et al., 2001).

124 The complex bedrock geology in the Torneträsk area consists of Archean plutonites (mainly
125 granite and syenite) and their metamorphic products that are overthrusted by Caledonian
126 metasediments and amphibolites (Swedish Geological Survey (SGU) database;
127 maps2.sgu.se/kartgenerator/maporder_sv.html). During the retreat of the Weichselian ice sheet,
128 the NW-SE trending Torneträsk depression hosted one/multiple ice-dammed lakes with water
129 levels up to 250 m higher than today as suggested by paleoshoreline and paleodelta deposits
130 (Gretener and Stromquist, 1981; Melander 1977). The area was largely deglaciated around 9500
131 cal yr BP (glaciers occupy ~0.5% of the watershed today (SMHI; https://vattenwebb.smhi.se/)),
132 leading to the drainage of the precursor lakes and the likely establishment of the present
133 shoreline. This approximate minimum deglaciation age is suggested by several radiocarbon-dated
134 sediments from smaller lakes within Torneträsk's catchment (e.g., Barnekow et al., 1998; Bigler
135 et al., 2003; Shemesh et al., 2001) as well as by cosmogenic radionuclide dating of glacially
136 scoured surfaces and erratics from the area (Stroeven et al., 2002). Bedrock is exposed or only
137 covered by thin soils (<1m) in large parts of the catchment (~43%; SMHI;

https://vattenwebb.smhi.se/), particularly at higher elevations in the mountains overlooking western Torneträsk, whereas glacial, glaciofluvial and fluvial deposits occur in confined areas at lower elevations. In lower lying areas, mires have developed in local depressions (Melander 1977; SGU database; maps2.sgu.se/kartgenerator/maporder_sv.html).

The climate in the Torneträsk area is generally oceanic but has a pronounced oceanic-continental gradient from W to E that is enhanced by the strong orographic effect of the Scandes Mountains (Table 1). Ice cover on the lake usually occurs from December/January to May/June. The Torneträsk area is located in the zone of discontinuous permafrost and catchment vegetation consists of alpine tundra above the present tree-line at 600–800 m a.s.l. and subalpine birch to northern boreal pine-birch forests below tree-line, with a total forest cover of ~18% across the watershed (SMHI; https://vattenwebb.smhi.se/). Pine has a continuous distribution in the SE part of the Torneträsk catchment, whereas pine occurs only sporadically in the western part of the catchment below 450 m a.s.l. Dwarf shrubs dominate the field layer vegetation together with grasses, sedges and herbs (Barnekow and Sandgren, 2001).

In addition to sediments from Torneträsk, we also recovered and analyzed a sediment sequence from Abiskojaure (68° 18' N, 18° 36' E; 488 m a.s.l.; Fig. 1) to provide a more comprehensive view on changes in catchment dynamics and aid in constraining the chronology of core Co1282 by cross-correlation (see 4.2.2 Chronology). Abiskojaure's watershed, located in the SW watershed of Torneträsk, is one of the main sub-watersheds (368 km^2) and drains via Abiskojåkka into the lake. The lake has a residence time of c. 0.2 years, a surface area of 2.8 km^2, an average and max. depth of 16.4 m and 35 m, respectively (SMHI; https://vattenwebb.smhi.se/). Birch forest occurs along the river corridor up to ~700 m a.s.l. and covers <10% of the watershed, while most of the watershed consists of sparsely vegetated alpine

tundra with thin soils (<1m) or unvegetated areas with exposed bedrock (~78% of the watershed). Glaciers cover about 1% of Abiskojaure's watershed (SMHI; https://vattenwebb.smhi.se/; SGU database; maps2.sgu.se/kartgenerator/maporder_sv.html).

Earlier paleoecological studies in the Torneträsk watershed did not identify distinguishable environmental impacts in response to human activities, which were likely minor and limited to fishing and hunting up to the 17th century when more intensive reindeer husbandry started to develop (Emanuelsson, 1987). During the past century, infrastructure developments in the area included railroad (built AD 1898-1902) and highway (built AD 1980-1984) construction along the southern shore of the lake.

Table 1. Meteorological data for three weather stations across the Torneträsk watershed (West to East) for the period 1961-1990 (http://www.smhi.se/klimatdata/meteorologi/temperatur/dataserier-med-normalvarden-1.7354). Winter is defined as the period October to April and summer as the period May to September.

Station		Katterjåkk	Abisko	Torneträsk
Latitude		68° 25'N	68° 21'N	68° 13'N
Longitude		18° 10'E	18° 49'E	19° 43'E
Altitude (m)		500	388	393
Precipitation (mm)	Annual	844	304	476
	Summer	340	157	268
	Winter	504	147	208
Temperature (°C)	Annual	–1.7	–0.8	–1.0
	Summer	+6.4	+7.5	+7.9
	Winter	–7.5	–6.8	–7.4

3. Material and methods

3.1 Sampling

Surface samples and a composite sediment core (Co1282) from Torneträsk were recovered from the ice-covered lake in April 2012. The surface samples were collected from 43 sites across the lake using a gravity corer (Fig. 2). The uppermost 2 cm were subsampled on site and stored in a freezer. Core Co1282 was sampled in the western lake basin at a water depth of 130 m (68° 23'40"N, 18° 50'55"E; Fig. 2). The sampling site was selected based on hydroacoustic data, which indicated the presence of acoustically stratified, horizontally continuous and extensive high and low amplitude reflections that are indicative of continuous hemi-pelagic sedimentation (Vogel et al., 2013) (Fig. S1). We recovered a 18.2-cm-long gravity core and a 181.2-cm-long percussion piston core at the coring site Co1282 using UWITEC equipment. The overlapping cores were correlated based on macroscopic lithological features such as red iron oxide and black manganese oxide layers and supported by geochemistry (major element concentrations, Si/Al and Pb/Ti ratios), which yielded a total composite core length of 188.2 cm. The sediment sequence from Abiskojaure was recovered in April 2016 using a gravity and piston corer and yielded a composite core length of 217.5 cm. Cores were stored at 4°C until subsampling in the laboratory.

3.2. Age-depth modeling

Several techniques were employed to date the composite core from Torneträsk, including ^{210}Pb, accelerator mass spectroscopy (AMS) radiocarbon, optically stimulated luminescence (OSL) dating, and, after difficulties with radiocarbon and OSL dating of the Torneträsk sediment, cross-correlating significant geochemical changes in the record to those recorded in the AMS macrofossil radiocarbon-dated sediment record from Abiskojaure. Near-surface sediments were radiometrically dated by analyzing ^{210}Pb, ^{226}Ra, ^{137}Cs and ^{241}Am by direct gamma assay in the Environmental Radiometric Facility at University College London. The resulting ^{210}Pb

chronology was calculated using the constant rate of ^{210}Pb supply (CRS) dating model (Appleby, 2001).

Terrestrial plant macrofossils are absent in core Co1282; thus AMS radiocarbon ages were determined on six bulk sediment samples at the LARA radiocarbon dating facilities of the University of Bern. Three plant macrofossils from the sediment record from Abiskojaure yielded sufficient C for AMS radiocarbon dating (Beta Analytic INC) (Table 2). All ages are reported as calibrated ages BP, i.e., before AD 1950 (cal yr BP). OSL dating was conducted on unexposed fractions of 10 cm half-core rounds in the OSL laboratory of the Institute of Geological Sciences at the University of Bern. Only polymineral fine grains were measured as the quartz fraction did not yield a luminescence signal. Both sample preparation and measurement were carried out as reported in Lowick et al. (2015), as was dose rate determination.

We used the IntCal13 calibration curve (Reimer et al., 2013) for calibration of radiocarbon ages and the Bayesian age-depth modeling software Bacon 2.2. (Blaauw and Christen, 2011) to determine the age-depth relationship in the sediment cores. The technique estimates accumulation rates by using Markov Chain Monte Carlo simulations and models age uncertainties for each sample interval in the core (Blaauw and Christen, 2011).

3.3. Geochemistry

Prior to analyses, all sediment samples were freeze-dried and ground using a swing mill for samples from Abiskojaure and core Co1282 and a planetary mill for the surface samples, respectively. Major and trace element geochemistry was measured on 0.2 g sample material by wavelength dispersive X-ray fluorescence using a Bruker S8 Tiger spectrometer equipped with an Rh anticathode X-ray tube. Precision was within ±3% for all elements used in this study except for Zr (±6%), and accuracy was within ±5% except for Na (±10%), Mg (±8%) and Zr

(±6%) (Rydberg, 2014). To infer compositional changes in the minerogenic fraction related to the degree of weathering, we used the K/Al ratio and the more comprehensive ratio $(Na_2O+MgO+K_2O+CaO)/TiO_2$. These ratios can provide information about the weathering degree of the detrital siliciclastics because the comparatively more mobile alkali and alkaline earth elements are preferentially leached from aluminosilicates compared with immobile Al or Ti during chemical weathering (cf., Kauppila and Salonen, 1997; Parker, 1970; Roy et al. 2008). The ratio $(Na_2O+MgO+K_2O+CaO)/TiO_2$ is hereafter referred to as the Chemical Index (CI), where lower values would indicate a more intensive chemical weathering. However, changes in these ratios must be interpreted with caution because they can also be influenced by, e.g., changes in grain-size or source of the deposited material (Boyle 2001). To assess potential concurrent changes in grain-size or source material and their potential influence on the CI, we used K/Rb and Zr/Ti ratios. K/Rb can provide information about grain-size changes because K is enriched in feldspars, which occur primarily in the coarser grain fraction, while Rb is common in micas and clays that are more abundant in the fine fraction. Lower ratios indicate finer-grained and higher ratios coarser-grained material (Kylander et al. 2013). Zr/Ti varies depending on the type of parent material, and has thus been used to identify possible changes in the source of material when assuming equal mobility of both elements during low-temperature weathering (Fabel et al. 2006; Kylander et al. 2013; Law et al. 1991; Reynolds et al. 2004).

Biogenic silica (bSi) in the sediment of Torneträsk was determined by Fourier transform infrared (FTIR) spectroscopy using a Bruker Vertex 70 equipped with a MCT (mercury-cadmium-telluride) detector, a KBr beam splitter, and a HTS-XT accessory unit (multi-sampler). 11 mg of sample material was mixed with 0.5 g of oven-dried spectroscopic grade potassium bromide (KBr) for the analysis. Quantifications are derived from a PLSR calibration model based on

246 synthetic sediment mixtures with defined bSi content. For more specific details about the method,
247 analytical procedure and instrument setup see Meyer-Jacob et al. (2014a). Total carbon (TC),
248 total nitrogen (TN) (from which we calculated atomic C/N- ratios), $\delta^{13}C$ and $\delta^{15}N$ were analyzed
249 using a Flash EA 2000 elemental analyzer coupled to an isotope ratio mass spectrometer (Thermo
250 Fisher Scientific). Samples were not treated with HCl prior to elemental analysis because FTIR
251 analyses showed that the samples did not contain inorganic carbon/carbonates, which have very
252 distinct FTIR spectral characteristics (cf., Rosén et al. 2011, Vogel et al. 2008). TC is therefore
253 considered as equivalent to total organic carbon (TOC). Element and bSi concentrations are
254 expressed as percentage by weight. Accumulation rates of bSi (AR_{bSi}; $g \cdot m^{-2} \cdot yr^{-1}$) were calculated
255 according to Eq. (1):

256 $$AR_{bSi} = SR \times DBD \times \%bSi \times 10^2, \quad (1)$$

257 where SR is the sedimentation rate ($cm \cdot yr^{-1}$), DBD is the dry bulk density ($g \cdot cm^{-3}$), and %bSi is
258 the bSi concentration of the sample.

259 Si/Al ratios, indicative of relative changes in bSi content (Peinerud et al. 2001), were used to
260 facilitate the cross-correlation of the records from Torneträsk and Abiskojaure in which bSi was
261 not quantified. In Torneträsk the correlation between bSi and Si/Al ratios is R^2=0.83.

262 3.4. Diatom analysis

263 Diatom slides were prepared using standard methods including digestion with 30% H_2O_2 as
264 described in Battarbee et al. (2001). Rinsed diatom samples were dried on coverslips and
265 permanently mounted onto microscope slides using Naphrax. Diatom identification followed
266 mainly Krammer and Lange-Bertalot (1986-91) and the guidelines of the Surface Water

Acidification Programme (SWAP) (Stevenson et al., 1991). For stratigraphical display, diatom counts are expressed as relative abundances.

3.5. Oxygen and silicon isotope analyses of diatom silica

Diatom samples for isotope analyses were purified following the cleaning stages described in Morley et al. (2004), which include removal of OM, sieving, differential settling and density separation. Prior to analyses, diatom sample purity was assured by visual inspection via SEM and by micro XRF measurements. $\delta^{18}O$ and $\delta^{30}Si$ were analyzed using a step-wise fluorination method. The outer hydrous layer of the diatoms was removed in a pre-fluorination stage using a BrF_5 reagent at low temperature. This was followed by a full reaction at high temperature to liberate oxygen (that was converted to CO_2 and measured for $\delta^{18}O_{diatom}$) and silicon (collected as SiF_4) isotopes that were measured using a MAT 253 dual-inlet mass spectrometer. $\delta^{18}O$ values were converted to the VSMOW scale and $\delta^{30}Si$ values were converted to the NBS28 scale, both using the within-run laboratory standard BFC_{mod}.

3.6. Interpolation of spatial variability

We used inverse distance weighted (IDW) interpolation in the ArcGis 10.2.1 software to interpolate and visualize the spatial variability of TOC, C/N ratios, bSi and the CI across Torneträsk.

4. Results and discussion

4.1. Spatial variability of recent sediment composition

TOC, atomic C/N ratios, bSi and the CI are shown in Figure 2 to exemplify the spatial variability in the surface sediments of Torneträsk. TOC concentrations are generally low, ranging from 0.2

to 5.3% (mean: 2.7%). C/N ratios vary from 10.2 to 17.1 (mean: 12.9), which suggests both aquatic and terrestrial OM (Meyers and Ishiwatari, 1993). bSi and the CI exhibit strong spatial variability with values in the ranges of 0–46.5% (mean: 14.6%) and 10.4–16.0 (mean: 11.9), respectively. Variations in the surface (i.e., recent) sediment composition are mainly controlled by i) the proximity to riverine input, ii) differences in catchment characteristics that result mainly from the contrasting landscapes in the western and eastern parts of the catchment, and iii) the heterogeneous bedrock geology. Close to river inlets such as Abiskojåkka, terrestrial-derived OM explains elevated C/N ratios and an increased riverine input of clastic material causes a dilution of TOC and bSi concentrations. Hydroacoustic measurements in Torneträsk indicate that sediment accumulation is up to 8 times higher in proximity to major river inlets compared to rates in distal areas; for example, the sediment thickness is >8 m near the Abiskojåkka inlet but less than 2 m in more distal parts of the western basin (Vogel et al., 2013).

In addition to proximity to river inlets, TOC, C/N ratios and bSi show differences from W to E across Torneträsk. When divided into a western (n = 29) and an eastern (n = 15) subset, mean TOC, C/N ratios and bSi values differ significantly between lake basins with 2.4 versus 3.4% TOC, C/N ratios of 13.5 versus 11.7, and 10.1 versus 23.3% bSi in the western and eastern half, respectively. This pattern can be explained by the likely different style and intensity of erosion and weathering in the western compared to the eastern watershed of Torneträsk. In the western watershed, higher relief energies, large areas of exposed bedrock and sparser vegetation cover would promote the erosion of chemically less-matured substrates. Similarly, low rates of microbially catalyzed weathering processes and OM turnover in soils would limit the release of nutrients and dissolved load. In contrast, the eastern catchment, with lower relief energies, thicker soils, a denser/more productive vegetation cover and more extensive peatlands, would favor an

312 enhanced release of nutrients/dissolved load. This is supported by several studies that show
313 increased silicate weathering rates and inorganic P release with increasing vegetation cover in
314 previously glaciated regions (Anderson et al., 2000; Humborg et al., 2004; Moulton et al., 2000).
315 These differences in catchment characteristics may explain the contrasting patterns of sediment
316 composition indicated by the proxies for aquatic production (bSi, TOC) and organic matter
317 source (i.e., C/N). The CI does not show a distinct spatial pattern in Torneträsk (Fig. 2), because
318 the mineral composition within the lake basin reflects not only the degree of weathering but also
319 the heterogeneity of the bedrock geology in the Torneträsk area.

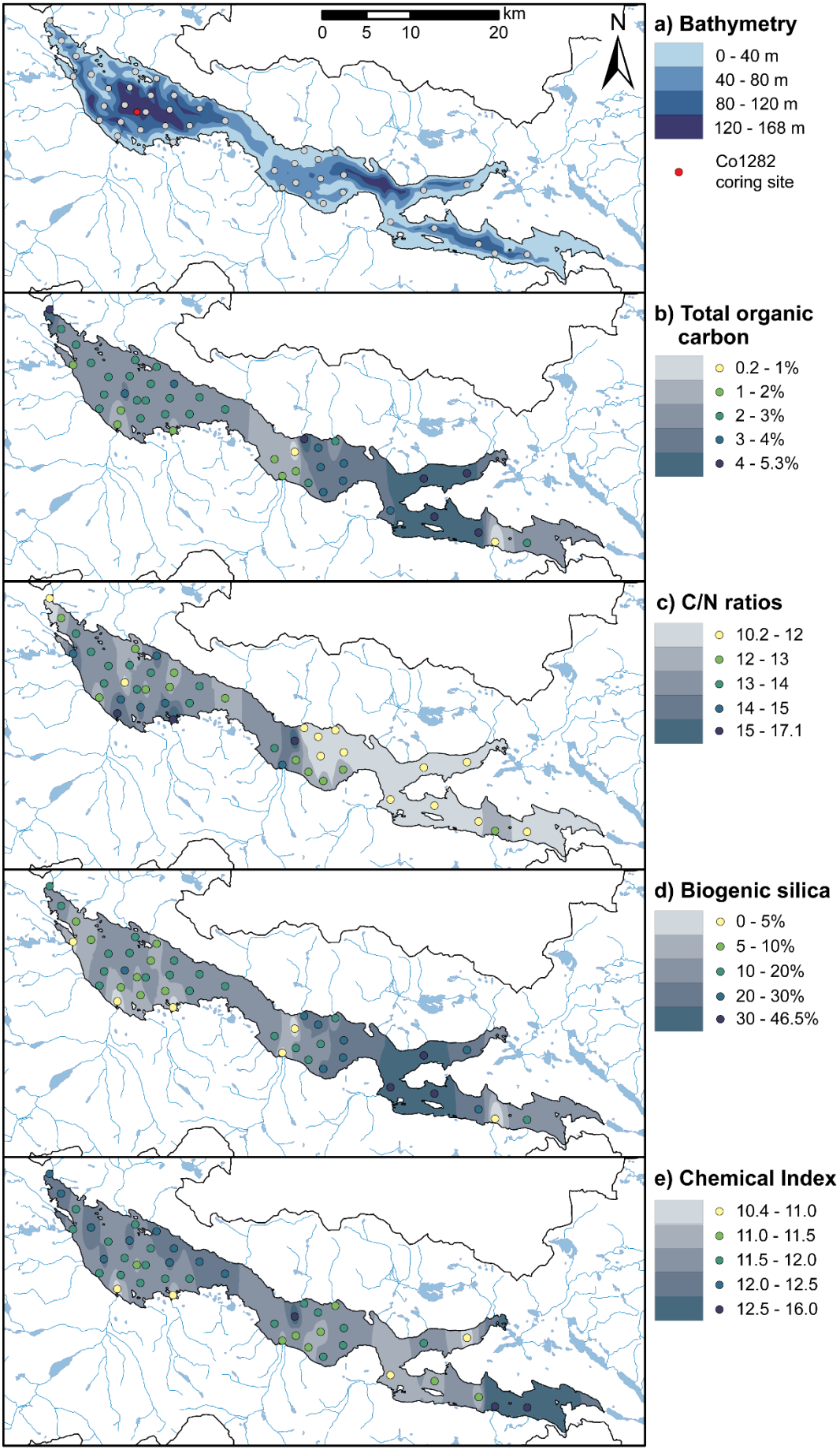
km
0 5 10 20
N
a) Bathymetry
0 - 40 m
40 - 80 m
80 - 120 m
120 - 168 m
Co1282
coring site
b) Total organic carbon
0.2 - 1%
1 - 2%
2 - 3%
3 - 4%
4 - 5.3%
c) C/N ratios
10.2 - 12
12 - 13
13 - 14
14 - 15
15 - 17.1
d) Biogenic silica
0 - 5%
5 - 10%
10 - 20%
20 - 30%
30 - 46.5%
e) Chemical Index
10.4 - 11.0
11.0 - 11.5
11.5 - 12.0
12.0 - 12.5
12.5 - 16.0

Figure 2a) Bathymetric map of Torneträsk with 40 m contour intervals based on bathymetric measurements from 1920/1921. b-e) Spatial variability of total organic carbon (TOC), C/N ratios, biogenic silica (bSi), and the chemical index (CI) in the surface sediment (0-2 cm) of Torneträsk. Color-coded dots indicate site-specific values, whereas contour lines were interpolated using IDW interpolation in ArcGis 10.2.1 and indicate interpolated ranges.

4.2 Long-term variations (core Co1282)

4.2.1 Lithology

The 188.2-cm-long sediment core Co1282 comprises a record of the depositional history in the western Torneträsk basin from the end of the Weichselian glaciation to the onset of lacustrine sedimentation until the present. The sequence can be subdivided into four lithofacies. The basal lithofacies A (188–178 cm blf; Fig. 3) is characterized by a grey, massive and dense matrix-supported diamicton with gravel and sand in a clay matrix. Due to its specific characteristics, particularly the high density of the material in combination with the glacigenic setting, we interpret the diamicton as a basal moraine deposit/lodgement till. The diamicton is overlain by lithofacies B (178–168 cm blf; Fig. 3), which is composed of unconsolidated and poorly sorted gravely-coarse sand and thus likely of glacio-fluvial origin. The following lithofacies C (168–117 cm blf; Fig. 3) appears thinly bedded and consists of light-grey clayey silt that is interrupted by normally graded layers of slightly coarser material (silt). This facies was likely deposited in a distal proglacial environment during the ice-dammed lake phase in the Torneträsk basin. The rhythmical lamination of the fine-grained sediments would result from variations in the sedimentation regime (suspension settling) due to fluctuations in intensity and sediment load of meltwater discharge coming from the retreating ice sheet (Carrivick and Tweed, 2013).

Lithofacies D (117–0 cm blf; Fig. 3) is characterized by homogenous silty clay with a color change from dark grey at the bottom to brown-grey towards the surface. Deposition of lithofacies D commenced after the retreat of the Fennoscandian ice sheet from the area and represents the continuous hemipelagic lacustrine sedimentation in Torneträsk during the Holocene. Between 15–7 cm blf, distinct horizons occur that consist of Fe-rich (up to 8.9%) reddish layers overlain by diffuse dark lenses rich in Mn (up to 2.5%; Fig. 3). Similar layers have been reported for sediments of other large, oligotrophic lakes, such as Lake Baikal where they have been ascribed to enrichment of redox sensitive elements at the redox front in low sedimentation rate settings (Och et al., 2012).

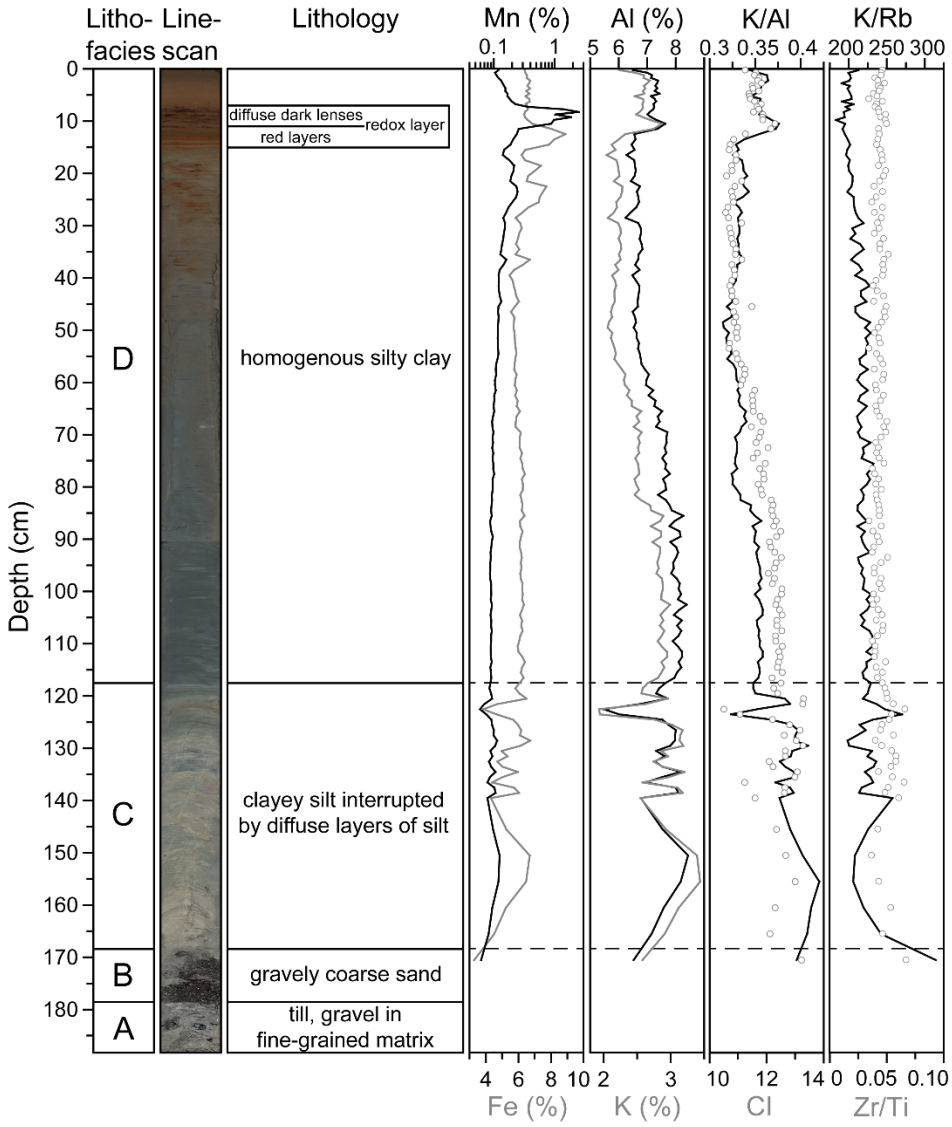

353

354 Figure 3. Lithofacies, color linescan, lithological description, and concentrations of Mn, Fe, Al,
355 and K, as well as the Chemical Index (CI) and K/Al, K/Rb, and Zr/Ti ratios for core Co1282,
356 recovered from the western basin of Torneträsk.

357

358 4.2.2 Chronology

359 The chronology of core Co1282 from Torneträsk is constrained by ^{210}Pb dating as well as cross-
360 correlating significant geochemical changes to those in the AMS radiocarbon-dated sediment

record from Abiskojaure (Figs. 4 and 5). Total ^{210}Pb activities in the sediment reached equilibrium with the background (supported) ^{210}Pb activity at 1.5–2 cm, which indicates a low sedimentation rate of ~0.015 cm·yr^{-1} in the near-surface sediments (Fig. 4a, b).

Radiocarbon measurements on bulk OC in core Co1282 suggest a large and variable reservoir/old carbon effect for bulk OC accumulated in the sediments of Torneträsk (Table 2). The surface sample (0–1 cm) and a near-surface sample (1.5–2 cm), which are within the ^{210}Pb dating range, yield ^{14}C ages of 2772±19 and 4533±22 yrs BP, respectively (Table 2). The large and variable reservoir effect is corroborated by radiocarbon dates determined in another core from the western basin of Torneträsk, which also range between 3580 and 5330 yrs BP in the investigated uppermost 18 cm of the core (Vonk et al., 2012). For the luminescence dating, gamma spectrometric measurements revealed a strong disequilibria in the U-Ra series for all samples, and suggest a later enrichment in U after deposition. In light of this, minimum and maximum ages were calculated using the dose rates determined using the activities of ^{238}U and ^{226}Ra, respectively (Table S1), and both sets of ages dramatically overestimate the expected ages for the core. This suggests that the luminescence signal was not fully zeroed prior to burial. The presence of a significant residual signal, together with the problem of disequilibrium over time in the radionuclides, makes it impossible to obtain reliable OSL ages.

Because of the large age overestimates obtained from both radiocarbon and luminescence dating, these results could not be used to constrain a robust age-depth relationship in core Co1282. Instead, to constrain the chronology we cross-correlated significant geochemical changes in core Co1282 with those clearly observed in the core from Abiskojaure for which a chronology was established based on AMS radiocarbon dated woody plant macrofossils (twig fragments) (Table 2, Fig. S2). Four sections with similar patterns of change across both sediment sequences can be

384 identified: 1) high CI values (>12) and low Si/Al ratios in deeper sediments: 82-117 cm in
385 Torneträsk and >184 cm in Abiskojaure; 2) declining CI from >12 to ~11, increasing bSi trend:
386 82-56 cm/184-104 cm (Abiskojaure's sediment composition is more variable during this period,
387 reflecting the coring location in close proximity to the inlet); 3) low CI (<11), high Si/Al: 56-12
388 cm/104-29 cm; and 4) in recent sediment a shift to higher CI (~11 or higher) and drop in Si/Al
389 12-0 cm/29-0 cm (Fig. 4). Only three macrofossils with sufficient C could be extracted from the
390 sediment core of Abiskojaure; however these macrofossils originate from sample levels at or near
391 the pronounced changes in geochemical properties recorded in Abiskojaure's sediments and thus
392 provide satisfactory age-depth control for the timing of major changes in the sediment
393 composition of Torneträsk. Similar geochemical changes in both cores suggest that the recorded
394 dynamics in core Co1282 are representative for the western Torneträsk catchment and/or
395 dominated by the riverine sediment input from Abiskojåkka, which drains Abiskojaure. Because
396 of the potential time lag that may exist for when the changes were recorded in Torneträsk and the
397 upstream-located Abiskojaure, inferred ages for core Co1282 based on the cross-correlation to
398 Abiskojaure should be considered as minimum ages.

399 We constrained the basal age for the lacustrine sediments (117 cm depth) in core Co1282 based
400 on radiocarbon-dated sediment records from small lakes in this area and cosmogenic exposure
401 ages of glacially-scoured surfaces and erratics, which indicate a deglaciation age around
402 9500±250 cal yr BP (e.g., Barnekow et al., 1998; Bigler et al., 2003; Shemesh et al., 2001;
403 Stroeven et al. 2002) (Fig. 4). This would imply an average Holocene sedimentation rate of 0.01
404 cm yr^{-1}, which is consistent with the recent sedimentation rate indicated by ^{210}Pb dating.

405

406 Table 2. Calibrated radiocarbon ages for the sediment sequences from Abiskojaure and

407 Torneträsk.

Laboratory ID	Sample ID	Composite depth (cm)	^{14}C age (yr BP)	Calibrated age range (2σ) (cal yr BP)	δ^{13}C	Material
Beta-440907	AJ2016In_K32-33	32.5	950 ± 30	930–790	–26.8	Woody plant macrofossil
Beta-440908	AJ2016In_P85.5	95	2200 ± 30	2320–2130	–27.4	Woody plant macrofossil
Beta-442326	AJ2016In_P175	184.5	5970 ± 30	6885–6735	–28.0	Woody plant macrofossil
2234.1.1	Co1282-1_0-1	0.5	2772 ± 19	2926–2795	–25.4	Org C
2633.1.1	Co1282-1_1.5-2	1.75	4533 ± 22	5310–5055	–32.0	Org C
2235.1.1	Co1282-1_16-17	16.5	4867 ± 23	5646–5588	–24.5	Org C
2236.1.1	Co1282-3I_29-30	36.5	6290 ± 23	7263–7171	–24.1	Org C
2237.1.1	Co1282-3I_53-54	60.5	8752 ± 28	9891–9613	–22.6	Org C
2238.1.1	Co1282-3III_93-94	100.5	15914 ± 57	19413–18988	–18.2	Org C

408

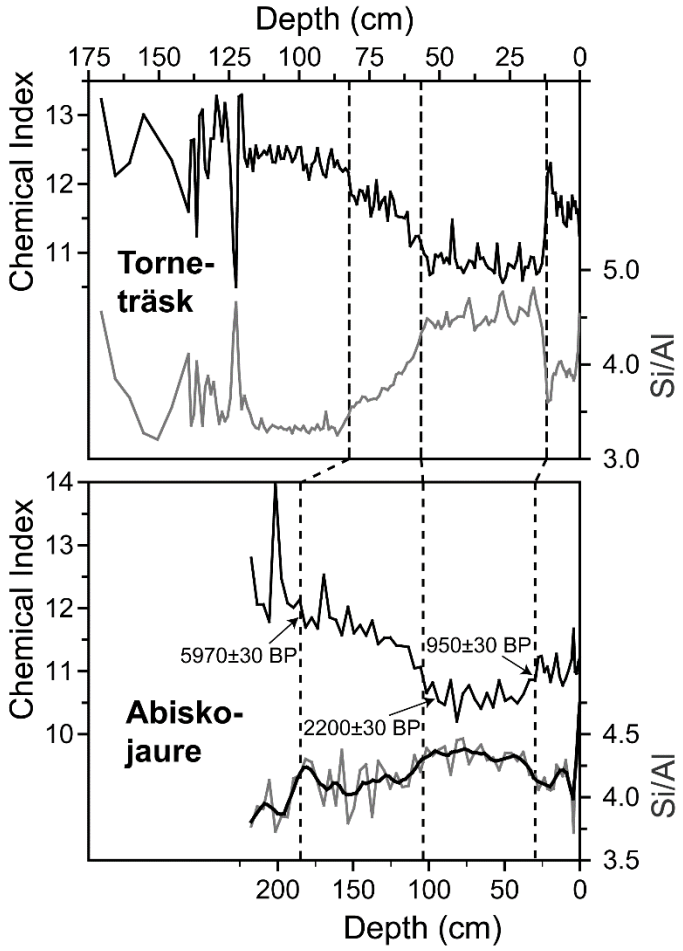

409

410 Fig. 4. Correlation between core Co1282 from the western Torneträsk basin and the core from
411 Abiskojaure using the chemical index and Si/Al ratios (note differences in x- and y-axis scaling
412 and range). Radiocarbon dates are given as ^{14}C ages (yr BP) and dashed lines indicate sections of
413 similar change used for correlating the two cores.

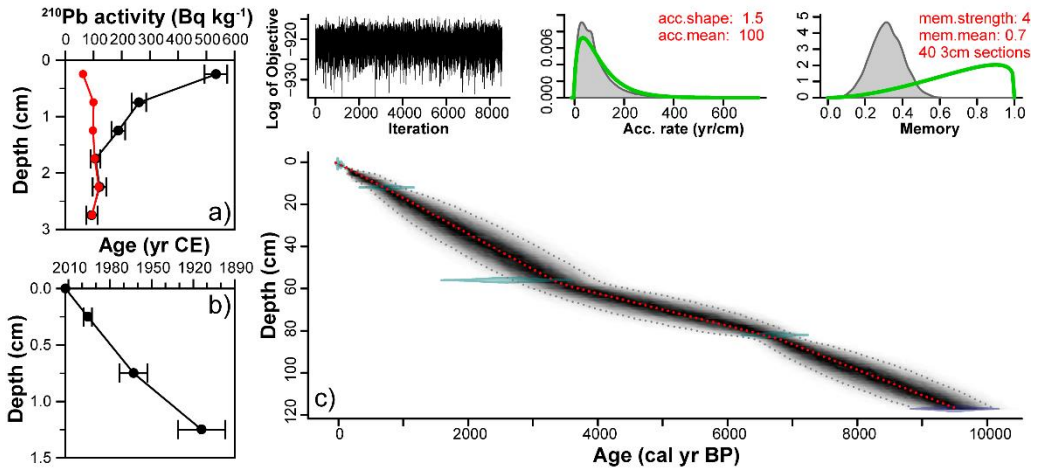

414

415 Figure 5. Chronology of core Co1282 from Torneträsk. a) Total (black) and supported (red) ^{210}Pb
416 concentrations versus depth. b) Radiometric chronology showing the CRS model ^{210}Pb dates. c)
417 Bayesian age-depth model based on ^{210}Pb-, dates inferred from the cross-correlation to the
418 radiocarbon-dated sequence from Abiskojaure (transparent green) and deglaciation age of the
419 area (transparent blue). 'Best' model based on the weighted mean age for each depth (red dashed
420 line) and 95% confidence intervals (grey dashed lines). Greyscale intensity indicates likelihood of
421 calendar ages. Upper panel (left to right) shows the Markov Chain Monte Carlo iterations (log of
422 objective), the prior (green curves) and posterior (grey histograms) distributions for the
423 accumulation rate and memory, respectively.

424

425 4.2.3 Holocene climatic and environmental development

426 <u>Ice-dammed lake phase (168–117 cm blf, lithofacies C)</u>

427 The proglacial sediments that accumulated in Torneträsk during its ice-dammed lake phase are
428 characterized by a highly variable geochemistry compared to the subsequent lacustrine
429 sediments. For example, major element concentrations fluctuate frequently between minimum
430 and maximum values of 3.3–6.7% for Fe, 1.9–3.4% for K, and 5.5–8.4% for Al (Fig. 3). The high

variability, corresponding to the rhythmical bedding/lamination of the proglacial sediments, is likely related to variations in grain-size, indicated by the K/Rb ratio ranging from 198 to 270, as a result of the varying intensity and sediment load of the meltwater discharge from the retreating ice sheet (Carrivick and Tweed, 2013).

Initial landscape development after deglaciation (117–84 cm blf; lithofacies D; ~9500–6600 cal yr BP)

The initial hemi-pelagic lacustrine sediments deposited after the deglaciation of the area show only minor compositional variations. Major element concentrations are stable with values around 2.9% for K and 8.0% for Al. Elemental ratios of K/Al, K/Rb, and Zr/Ti as well as the CI remain constant throughout this period with values around 0.35, 221, 0.042 and 12.4, respectively (Figs. 3 and 6). bSi concentrations are continuously low (<0.1%), which is consistent with a very low diatom abundance that in turn shows a stable diatom community composition (Fig. 7). Proxies associated with OM exhibit slight increases from 0.4 to 0.7% for TOC, from 0.03 to 0.05% for TN, from ~16 up to 18 for C/N ratios, and from +2.7 to +3.8‰ for $\delta^{15}N$, whereas $\delta^{13}C$ decreases from –22.1 to –23.2‰ (Fig. 6). In the corresponding sediment section from Abiskojaure, the CI is also high and relatively stable (~12) except for three samples associated with two clay layers (Fig. 4).

The constant major element concentrations, elemental ratios, and CI indicate that there are no qualitative changes in the composition of the minerogenic matter input from the catchment during the early Holocene. For example, the high CI is similar to the mean value of the proglacial sediments (12.5), which shows that the minerogenic material deposited during this period is essentially chemically unaltered. These data indicate a homogeneous sediment source, relatively

low chemical weathering rates and the presence of easily erodible and chemically unaltered glacigenic deposits in the Torneträsk area. Low weathering rates would limit the release of DSi and other nutrients into the aquatic system, and explain the low bSi concentrations and low diatom abundance in this part of the record.

The slight increase in C/N indicates a gradually increasing export of terrestrial OM into the lake, which would result from the gradual development of vegetation cover and soil formation in the catchment. This initial landscape development would similarly explain the observed trends for TOC, TN, $\delta^{15}N$ and $\delta^{13}C$. Conclusive interpretations of the $\delta^{13}C$ and $\delta^{15}N$ trends are complicated by the complex nature of bulk OM isotope signals (Meyers and Ishiwatari, 1993; Meyers, 2003) and the low magnitude of change of ~2‰ throughout the early and mid-Holocene; however Hammarlund (1993) and Hammarlund et al. (1997) suggested that early Holocene declines in $\delta^{13}C$ were the result of the transition from a deglaciated, vegetation-free landscape to tundra and finally forest vegetation during the initial landscape development. The authors proposed that the development of vegetation and soils enhanced soil respiration, which led to an increased export of ^{13}C-depleted carbon dioxide to the aquatic system and subsequently to a ^{13}C-depletion in phytoplankton.

Altered soil biogeochemical processes in response to a gradual development of vegetation cover would likewise account for the increase of $\delta^{15}N$ in core Co1282. In general, bulk OM $\delta^{15}N$ increases in soils with depth and OM age, which has been shown for soil profiles in the Torneträsk area (Makarov et al., 2008). During decomposition, the heavier ^{15}N is gradually enriched in the residual OM by isotopic fractionation (Högberg, 1997). Correspondingly, the increasing $\delta^{15}N$ trend in core Co1282 would result from enhanced soil OM decomposition and

476 increased leaching of ^{15}N-enriched nitrate in the course of progressing soil and vegetation

477 development in the Torneträsk catchment.

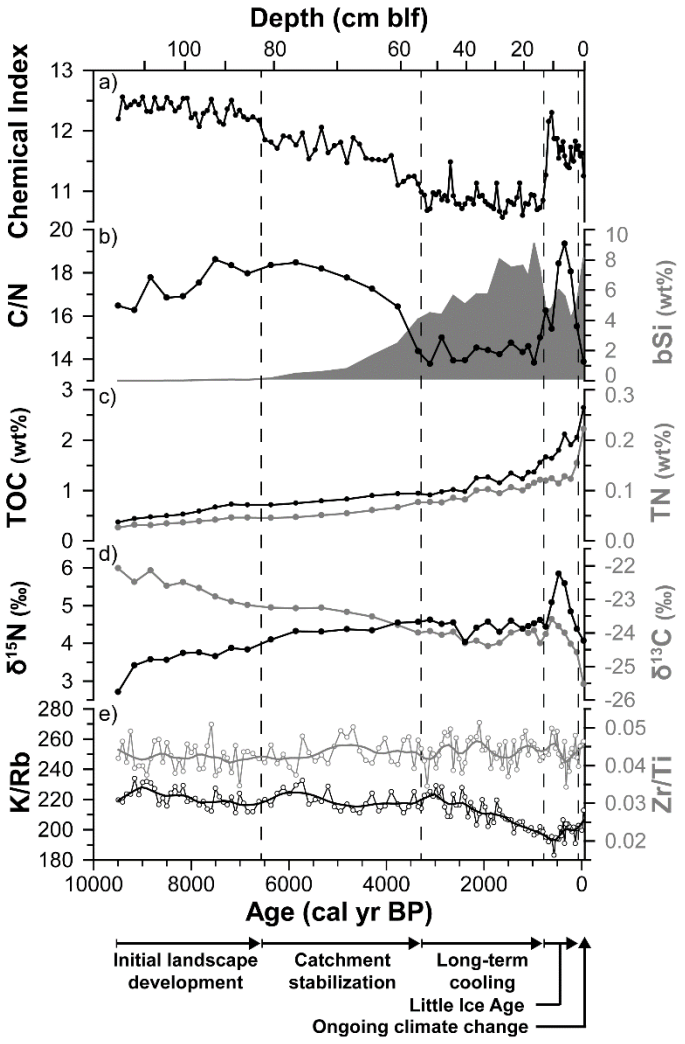

478

479 Figure 6. a) Chemical Index (CI), b) biogenic silica (bSi) and C/N ratios, c) total organic carbon

480 (TOC) and nitrogen (TN), d) $\delta^{13}C$, and $\delta^{15}N$, and e) K/Rb and Zr/Ti ratios versus inferred

481 sediment ages for core Co1282 from Torneträsk over the Holocene.

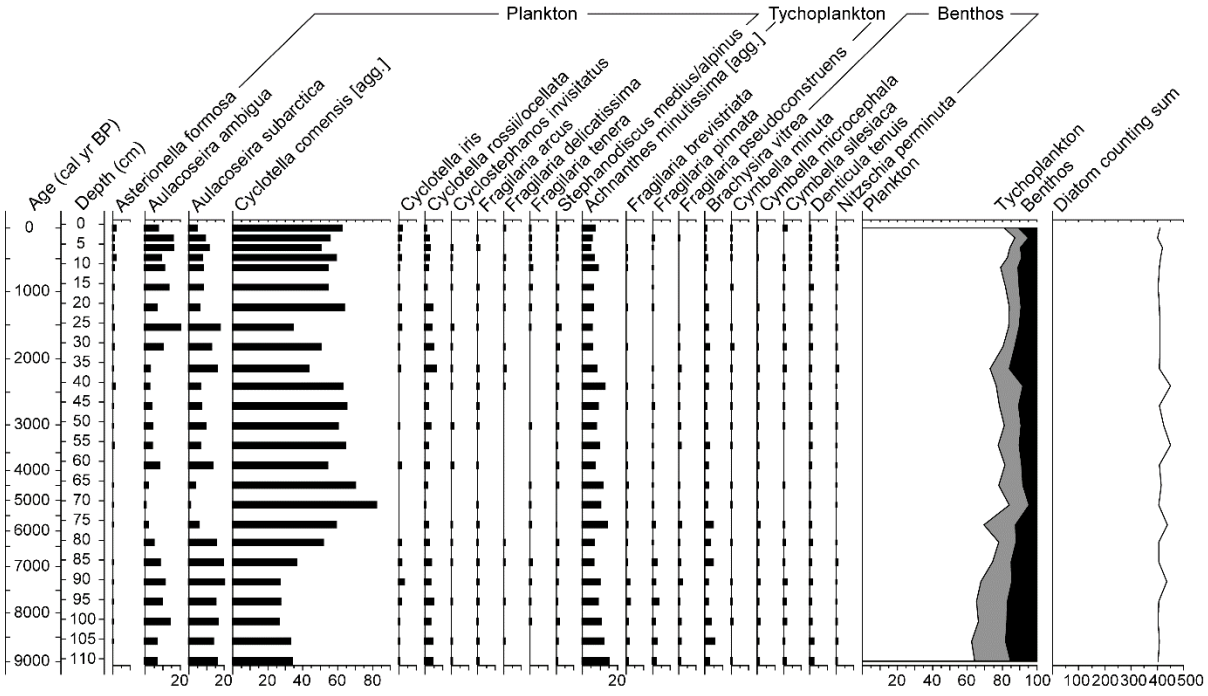

Figure 7. Relative abundance of selected diatom taxa for core Co1282 from Torneträsk over the Holocene. The scale at the base of each panel is given in percentages.

<u>Mid-Holocene thermal maximum and catchment stabilization (84–57 cm blf; lithofacies D; ~6600–3400 cal yr BP)</u>

Compared to the relatively uniform composition of the early Holocene sediments, the sediment composition gradually changed between ~6600 and ~3400 cal yr BP. Approximately 3000 years after deglaciation, concentrations of K and Al started to progressively decline from ~2.9 to ~2.2% and from ~8.0 to 6.8%, respectively. Simultaneously, K/Al ratios and CI decreased from ~0.35 to ~0.33 and from ~12.2 to 11.2, while K/Rb and Zr/Ti ratios remained stable with values fluctuating around 219 and 0.043, respectively (Figs. 3 and 6). bSi levels slowly increased from <0.1 to ~2%, whereas C/N ratios decreased from ~18 to 14.4. Other proxies associated with OM follow their early Holocene trends and continuously increased from 0.7 to 1.0% for TOC, from

0.05 to 0.08% for TN, and from +3.8 to +4.5‰ for $\delta^{15}N$, while $\delta^{13}C$ continued to decrease from –23.2 to –24.0‰ (Fig. 6). The CI in the sediment record from Abiskojaure likewise declined during this period from ~12 to ~11.4 (Fig. 4).

The distinct declines in K/Al ratios and CI indicate a qualitative change in the sediment composition that is likely driven by the depletion of mobile alkali and alkaline earth elements through chemical weathering of mineral matter in catchment soils because elemental ratios indicative for changes in grain-size (K/Rb) and source area (Zr/Ti) remained unchanged during this period. Studies from Lake Kilpisjärvi, northern Finland (Kauppila and Salonen, 1997), and from NW America (Whitehead et al., 1989) demonstrated that increased chemical weathering rates (and a loss of more mobile elements) followed the establishment of denser forests in previously glaciated areas. We therefore assume that the qualitative geochemical changes in core Co1282 are likewise driven by the widespread establishment of denser pine-birch forests, which commenced at ~7600 cal yr BP and reached maximum density during the HTM at ~6300 cal yr BP in the western Torneträsk catchment (Barnekow, 2000; Barnekow and Sandgren, 2001). The climate optimum during the HTM (~8000–4800 cal yr BP), with temperatures 1.5-2.0 °C warmer in northern Fennoscandia than at present (Barnekow, 2000; Barnekow and Sandgren, 2001, Seppä et al., 2009) (Fig. 8), also had an impact on in-lake processes and the diatom community composition in Torneträsk. The diatom assemblage shows a gradual shift with an increased abundance of *Cyclotella comensis* and decrease in *Aulacoseira ambigua* and *subarctica* (Fig. 7) likely in response to elevated temperatures during this period. Warming and earlier ice break-up may enhance the strength and duration of thermal stratification, which favors more buoyant *Cyclotella* taxa over heavier *Aulacoseira* taxa (Rühland et al., 2015). Bigler et al. (2006) found a similar shift in the diatom community in the small lake Vuolep Njakajaure (Fig. 1 F); however,

519 this shift occurred ~1000 years earlier, which indicates the slower (delayed) response to climate
520 change in the large and deep Torneträsk as also shown for other (sub)arctic lakes (Rühland et al.,
521 2015 and references therein).

522 The proceeding catchment transformation from bare bedrock and glacigenic sediment deposits
523 after deglaciation to a forested catchment supporting soil formation during the mid-Holocene is
524 corroborated by the consistent trends of $\delta^{15}N$ and $\delta^{13}C$, assuming that biogeochemical processes
525 in soils primarily control trends in stable C and N isotopes in the Torneträsk sediment during the
526 early lake development (cf., Hammarlund, 1993; Hammarlund et al., 1997; Wolfe et al., 1999).

527 Rather than indicating a decreased input of terrestrial OM into the lake, the decline of C/N ratios
528 together with the concurrent increase of bSi levels shows an increased importance of aquatic OM
529 production. This onset of notable aquatic production was facilitated by the increased export of
530 nutrients from the catchment following the vegetation development in the catchment and
531 subsequent intensification of chemical weathering. Likewise in Lake Kilpisjärvi, northern
532 Finland, initial bSi concentrations were low and did not significantly increase until the expansion
533 of pine and establishment of denser vegetation (Kauppila and Salonen, 1997). This is consistent
534 with watershed studies from northern Sweden, which show that fluxes of DSi in rivers increase
535 with increasing vegetation cover in the catchment (Humborg et al., 2004).

536 Changes in the availability of DSi can be traced using Si isotope analyses of diatom silica. In core
537 Co1282, we could extract sufficient material for diatom isotope analyses from 76 cm blf (~6000
538 cal yr BP) upwards when bSi concentrations were ≥0.2%. $\delta^{30}Si_{diatom}$ decrease from +0.37 to 0‰
539 between c. 6000 and 3000 cal yr BP, followed by lower values fluctuating around 0‰ (min: –
540 0.10, max: +0.15‰) during the remainder of the late Holocene until present (Fig. 8). Diatoms
541 preferentially incorporate ^{28}Si compared to ^{30}Si (and ^{29}Si), and consequently with enhanced

productivity and utilization of DSi, $\delta^{30}Si$ ($^{30}Si/^{28}Si$) progressively increases in the DSi pool. This productivity signal is recorded in the $\delta^{30}Si$ of diatoms because diatoms then incorporate DSi from this progressively ^{30}Si-enriched pool. Variations in the DSi supply can also alter the $\delta^{30}Si$ signal of diatoms by affecting the biological DSi demand (Leng et al., 2009; Swann et al., 2010). In the sediments of Torneträsk, the initial $\delta^{30}Si_{diatom}$ decline indicates increased DSi utilization during the earlier lake development. Because diatom productivity was very low during this period, we interpret the increased utilization as an indication for a higher DSi demand that resulted from the initially low weathering rates and thus low DSi supply. This suggests that diatom productivity in Torneträsk was Si limited during the early lake ontogeny, which delayed the onset of notable diatom production by ~3000 years after deglaciation until vegetation development facilitated Si export. Alternatively, an increase in weathering rates could also contribute to the initial $\delta^{30}Si$ decline; for example, Opfergelt and Delmelle (2012) found that $\delta^{30}Si$ decreased in soil profiles with increasing weathering degree.

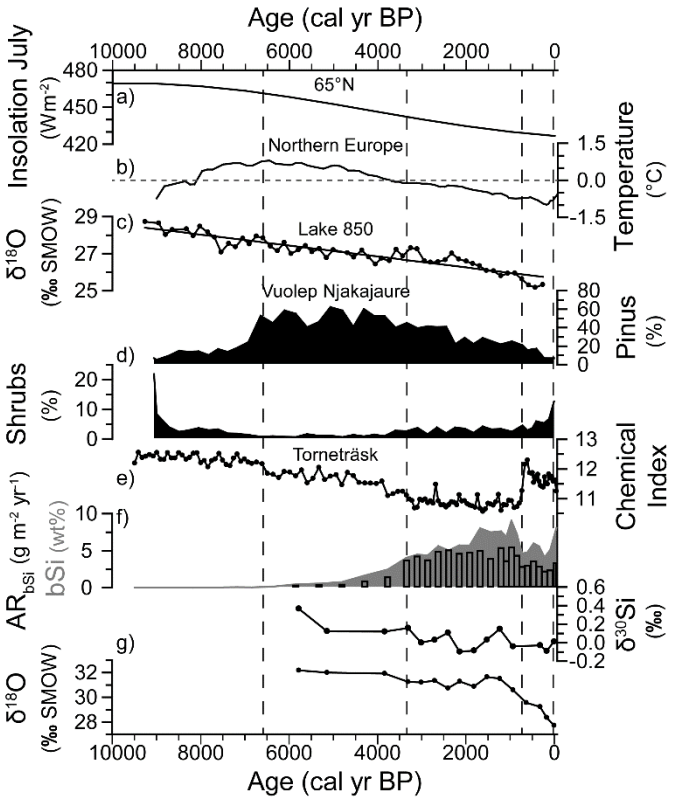

555

556 Figure 8. a) July Insolation at 65°N (Berger and Loutre, 1991), b) LOESS smoothed (span: 0.05)
557 stacked summary curve of the pollen-based temperature variability for Northern Europe (Seppä et
558 al., 2009), c) $\delta^{18}O_{diatom}$ for Lake 850 (Fig. 1 I, Shemesh et al., 2001), percentage terrestrial pollen
559 from d) *Pinus sylvestris* and shrub vegetation in the sediment record of Vuolep Njakajaure (Fig. 1
560 F; Barnekow, 2000) compared to e) the Chemical Index (CI), f) biogenic silica (bSi)
561 concentrations and accumulation rates (AR_{bSi}), g) diatom $\delta^{18}O$ and $\delta^{30}Si$ in the sediment core
562 Co1282 from Torneträsk over the past 6000 and 10000 years, respectively.

563

564 <u>Late Holocene climate cooling (57–13 cm blf; lithofacies D; ~3400–750 cal yr BP)</u>

565 Following the long-term vegetation expansion and catchment stabilization during the mid-
566 Holocene, most organic and inorganic geochemical properties in core Co1282 show no major

567 variations between ~3400 and 750 cal yr BP. Major element concentrations, K/Al and Zr/Ti
568 ratios as well as the CI fluctuate around 2.2% for K, 6.6% for Al, 0.33 for K/Al, 0.044 for Zr/Ti,
569 and 10.9 for CI (Fig. 3). C/N ratios, $\delta^{13}C$, and $\delta^{15}N$ are relatively stable during this period with
570 values around 14.4, –24.1‰, and +4.5‰, respectively, while TOC and TN concentrations
571 continued to increase slightly from 1.0 to 1.6% and from 0.08 to 0.12%, respectively (Fig. 6). In
572 contrast, bSi increased from 2 to above 7% over the whole period, whereas K/Rb ratios started to
573 decline around 2200 cal yr BP from values around 220 during the early and late Holocene to
574 ~200 by ~750 cal yr BP. Fe and Mn co-vary during this part of the sediment record and layers
575 enriched in Fe and Mn are most likely buried relicts of the active redox horizon that continually
576 moves upward with progressing sediment accumulation (Och et al., 2012) (Fig. 3). The CI in the
577 corresponding sediment section from Abiskojaure reached its lowest values during the Holocene
578 and stabilized around 10.7 (Fig. 4).

579 The relatively constant sediment geochemistry between ~3400 and 750 cal yr BP indicates no
580 larger changes in the composition of the catchment-derived sediment delivered to the coring site
581 in the western lake basin. In comparison, studies of smaller lakes at higher altitudes in the
582 catchment suggest increased soil erosion during the late Holocene from 3200–2600 cal yr BP
583 onwards, respectively (Berglund et al., 1996; Snowball and Sandgren, 1996; Rubensdotter and
584 Rosqvist, 2003). For the late Holocene, several paleolimnological studies in the Torneträsk area
585 indicate a climate cooling that led to a tree-line retreat, which would expose previously forested
586 soils and thus facilitate soil erosion. Pollen and macrofossil records indicate a lowering of the
587 pine tree line by ~175 m and also of mountain birch already from ~4500 cal yr BP, which is
588 assumed to represent a decline of the growing season temperature of ~1.5-2°C compared to
589 today. This tree-line retreat ultimately led to the establishment of today's more sparse subalpine

birch forests and an increased presence of dwarf shrubs, grasses and sedges across the landscape also at lower altitudes (Barnekow, 1999, 2000) (Fig. 8). Temperature reconstructions based on diatoms, chironomids and pollen likewise indicate a pronounced cooling during the late Holocene by ~1-2°C, but depending on the site and the chosen biological indicator the timing of the cooling onset varies between ~3500 and 1900 cal yr BP (Bigler et al., 2002; 2006). These landscape dynamics agree well with the proposed neoglacial expansions of the Kårsa glacier (Fig. 1 B) around 3300 cal yr BP (Berglund et al., 1996; Snowball and Sandgren, 1996) and of the Kalanvare glacier, located just outside the Torneträsk catchment (Fig. 1 A), at c. 4400, 3000, 2000, and after 1200 cal yr BP (Rosqvist et al., 2004). Increased glacial activity would increase production of finer-grained material (rock flour), which would ultimately be accumulated in Torneträsk. Declining K/Rb ratios in core Co1282 indicate such an increased contribution of finer-grained material from ~2200 cal yr BP onwards. This trend is corroborated by grain-size analyses from a short core that was recovered close to the coring site of core Co1282, which shows an increasing clay content over the corresponding depth interval (Vonk et al. 2012).

The continuous increase of bSi concentrations during this period would suggest a progressive improvement of environmental conditions for aquatic production but accumulation rates of bSi reveal instead that diatom production reached a somewhat stable level with AR_{bSi} around 4.5±1 $g \cdot m^{-2} \cdot yr^{-1}$ after the initial increase (Fig. 8). The overall low AR_{bSi} in Torneträsk is of the same order of magnitude as those reconstructed for other large lakes such as Lake Baikal (Qiu et al., 1993) or Lake El'gygytgyn (Meyer-Jacob et al., 2014b) in Siberia. Regardless of changes in bSi content and flux there was no significant change in the diatom assemblage (Fig. 7).

Soil erosion during the Little Ice Age (13–1 cm blf; lithofacies D; ~750-50 cal yr BP)

The relatively stable sediment geochemistry during the late Holocene was interrupted by a pronounced shift in the sediment composition commencing at ~750±275 cal yr BP contemporaneous with the beginning of the LIA (Matskovsky and Helama, 2014; Melvin et al., 2012; Seppä et al., 2009). Major element concentrations, K/Al ratios, and the CI shifted to higher values of ~2.6% for K, ~7.2% for Al, ~0.36 for K/Al, and ~11.7 for the CI, while Zr/Ti and K/Rb show no major changes and remain around 0.043 and 200, respectively (Fig. 3). bSi concentrations dropped to ~5%, whereas C/N ratios and $\delta^{15}N$ increased to maximum values of 19.4 and +5.8‰. $\delta^{13}C$ slightly increases only initially to –23.6‰ and drops to Holocene minimum values of –25.5‰ at the sediment surface, while TOC and TN follow their Holocene trend and reach maximum values of 2.6 and 0.22% in the most recent sediment (Fig. 6). In the corresponding sediment from Abiskojaure, the CI also shifted to significantly higher values (~11.1) (Fig. 4).

Elevated K/Al ratios and CI, together with constant Zr/Ti and K/Rb ratios, indicate a stable grain-size distribution and sediment source but that the minerogenic material deposited in Torneträsk from ~750 cal yr BP onwards is less-intensively weathered compared to sediment that accumulated since the beginning of the late Holocene cooling. Less-weathered material would come from deeper mineral soil layers, and together with an increase in C/N ratios indicating more terrestrial OM, this signifies enhanced soil erosion in the Torneträsk area. An enhanced erosion of catchment soils is also supported by the simultaneous increase of $\delta^{15}N$ in the sediment because OM from deeper soils is enriched in ^{15}N (Högberg, 1997); for example, Makarov et al. (2008) showed that deeper soil horizons (>10 cm soil depth) in the Abisko area exhibit $\delta^{15}N$ of >+5‰.

During the LIA, temperatures were ~1 °C cooler than at present in Fennoscandia with coldest tree-ring inferred summer temperatures during the 13th through 19th centuries for the Torneträsk

area (Matskovsky and Helama, 2014; Melvin et al., 2012; Seppä et al., 2009) (Figs. 8 and 9). Paleoecological temperature reconstructions from smaller lakes in the Torneträsk watershed likewise suggest a ~1 °C cooling over the last millennia (e.g., Bigler et al., 2002, 2003; Hammarlund et al., 2002). The pronounced cooling during this period is emphasized by the formation of permafrost in the area after 700 cal yr BP (Kokfelt et al., 2010; Rydberg et al., 2010). Neo-glacial activity also increased over the last millennium until the end of the LIA (Rosqvist et al., 2004; Snowball and Sandgren, 1996), which is reflected in the Torneträsk record by a higher input of finer-grained material indicated by the lowest K/Rb ratios recorded for the Holocene during this period (Fig. 6). However, increased glacial activity alone cannot explain the change in sediment composition during the LIA because, while increased glacial erosion would have exposed less-weathered material, it would not have altered the quality of the catchment-derived OM.

Carbonate and diatom silica $\delta^{18}O$ from several small-lake records in the study region indicate changes in atmospheric circulation patterns over the Holocene, and particularly during the late Holocene (e.g., Rosqvist et al., 2004, 2007; Shemesh et al., 2001). In the sediment sequence from Torneträsk, $\delta^{18}O$ in diatom silica declined by 4.5‰ during the past ~6000 years. The $\delta^{18}O$ decline was relatively slow between ~6000 and 750 cal yr BP with a total decrease of ~1.5‰, but accelerated substantially during the past ~750 years when $\delta^{18}O$ declined by an additional ~3‰ (Fig. 8). The successive long-term decline over the Holocene has been ascribed to changes in the relative contribution of different air masses to the area, changing from a maritime climate with a strong zonal airflow from W/SW to a more continental climate with a dominant meridional airflow from N/NE (Hammarlund et al., 2002; Shemesh et al., 2001).

Compared to the slight decline (1.5‰) over most of the Holocene, the strongly amplified decline (3‰) in diatom $\delta^{18}O$ during the past ~750 years requires a more significant change in climate. The main factors controlling diatom $\delta^{18}O$ are lake-water temperature and the $\delta^{18}O$ composition of the ambient lake-water, which in turn depends on the $\delta^{18}O$ composition of the local precipitation and evaporation. Several studies from smaller lakes in the Torneträsk area have suggested that temperature could not be the sole driver of the observed $\delta^{18}O$ changes and that a 1°C temperature decline, as indicated for the LIA, alone would have caused a $\delta^{18}O$ decline of <1‰ (e.g., Hammarlund et al., 2002; Rosqvist et al., 2013; Shemesh et al., 2001). Reduced evaporation could amplify the $\delta^{18}O$ decline, but lake-water surveys show that lakes in the area are generally little affected by evaporation (Jonsson et al., 2009); furthermore, lake-water $\delta^{18}O$ and $\delta^{2}H$ values from Torneträsk itself (Shemesh et al., 2001) fall on the local meteoric water line established by Jonsson et al. (2009), which indicates that the lake is – at least at present – unaffected by evaporation.

Changes in the $\delta^{18}O$ of precipitation is likely the most critical factor in the Torneträsk watershed and could have contributed to the pronounced $\delta^{18}O$ decline during the past ~750 years in two ways; one is an even stronger dominance of ^{18}O-depleted air masses, while the other is a relative increase in winter precipitation, which is more ^{18}O-depleted compared to summer precipitation due to the temperature difference during condensation (Dansgaard 1964). Each of these has been proposed by different paleoecological studies in the area. Rosqvist et al. (2004; 2007) suggested that lake-water $\delta^{18}O$ declined during periods dominated by dry and cool arctic air masses from N, leading to cooler summers. For the LIA, Loader et al. (2013) inferred an increased contribution of arctic air leading to cool and sunny summers from tree-ring based temperature and sunshine reconstructions for the Torneträsk area (Fig. 9).

Alternatively, Jonsson et al. (2010) suggested that increased winter precipitation and elevated winter/summer precipitation ratios led to a $\delta^{18}O$ decline in a high-altitude alpine lake record in the Torneträsk catchment. However, precipitation reconstructions for the study region exhibit mixed results (Hammarlund et al., 2002; Seppä and Birks, 2001). Lower summer temperatures as well as increased winter precipitation could both contribute to neo-glaciation, which has been observed during the LIA in Fennoscandia as well as specifically in the Torneträsk area (Karlén 1988; Nesje 2009; Rosqvist t al., 2004; Snowball and Sandgren, 1996).

Amplified climate change during the LIA is corroborated in the Torneträsk record by the simultaneous decline of AR_{bSi} (Fig. 8). Diatom production is sensitive to changes in the length of ice cover (Lotter and Bigler, 2000), which depends on the temperature (Magnuson et al., 2000) as well as the amount and timing of snowfall. Monitoring data since the early 20th century indicate that the ice-cover duration of Torneträsk is primarily driven by temperature. From 1913 to 2006, the mean ice-cover duration of Torneträsk decreased by ~40 days. Simultaneously, mean annual air temperatures have increased by 2.5°C at the Abisko research station, whereas snow depth initially increased but then declined since the 1980's (Callaghan et al., 2013). The increasing length of the open water season over the past 100 years, together with increasing temperatures, would explain the recent increase in bSi and AR_{bSi} (Figs. 6 and 8). The overall good agreement between bSi variations in the sediment record and tree-ring based changes in temperature and atmospheric circulation emphasizes the climate sensitivity of diatom production in Torneträsk during the past millennium (Fig. 9), which, however, did not significantly alter the diatom assemblage composition (Fig. 7).

Remarkably, the pronounced shift in sediment composition in Torneträsk did not occur until the start of the LIA despite an already ongoing climate cooling for more than 2000 years. In addition,

the abrupt nature of these changes in the sediment record indicates either a rather sudden change of environmental conditions with the onset of the LIA or alternatively that environmental conditions crossed a critical threshold in the Torneträsk watershed when temperatures further declined during the LIA. Climate reconstruction for the Torneträsk region indicate that the scale of climate change during the LIA was not unprecedented during the late Holocene. For example, no qualitative changes in the deposited sediments occurred in response to the gradual 1-2°C decline since the HTM or in response to a temperature decline of equal magnitude to the LIA during a cold period ~1400 cal yr BP (Matskovsky and Helama, 2014; Seppä et al., 2009) (Figs. 8 and 9).

Sediment records from smaller lakes in the Torneträsk catchment indicate increased mobilization of minerogenic matter already from 3400-2600 cal yr BP onwards, following tree-line retreat as well as increasing glacial activity during the late Holocene (Berglund et al., 1996; Rubensdotter and Rosqvist, 2003; Snowball and Sandgren, 1996). Similarly, increased soil erosion has been reported for higher elevation lakes in other parts of the Scandinavian Mountains following the late Holocene tree-line retreat (Barnett et al, 2001; Hammarlund et al. 2004). In contrast, increased erosion of catchment soils is not recorded in sediments of Torneträsk's western basin before the onset of the LIA when pollen records from the area show an increasingly open landscape, indicated by the further increased presence of dwarf shrubs, grasses and sedges (Barnekow, 1999, 2000; Bigler et al., 2002) (Fig. 8). The increasingly sparse vegetation cover would have further increased the susceptibility of soils to erosion, which are generally thin (~1 m), poorly developed, and have relatively shallow organic horizons (<15 cm) above the modern tree-line in the Torneträsk area (Darmody et al. 2004; Makarov et al. 2008). This is supported by radiocarbon-dated buried soils from the catchment that suggest highest deposition rates of

upslope eroded material during the LIA (Darmody et al. 2004). We propose that, following the tree-line retreat, catchment destabilization and subsequent soil mobilization occurred first mainly locally at higher elevations. With diminishing vegetation cover, the Torneträsk catchment gradually became more sensitive to soil erosion through, e.g., rainfall events and snowmelt run-off, and crossed a critical threshold around ~750 cal yr BP. From that time onwards, previously forested soils in large parts of the catchment were increasingly exposed to erosion and less-weathered material was also transported into Torneträsk's western basin.

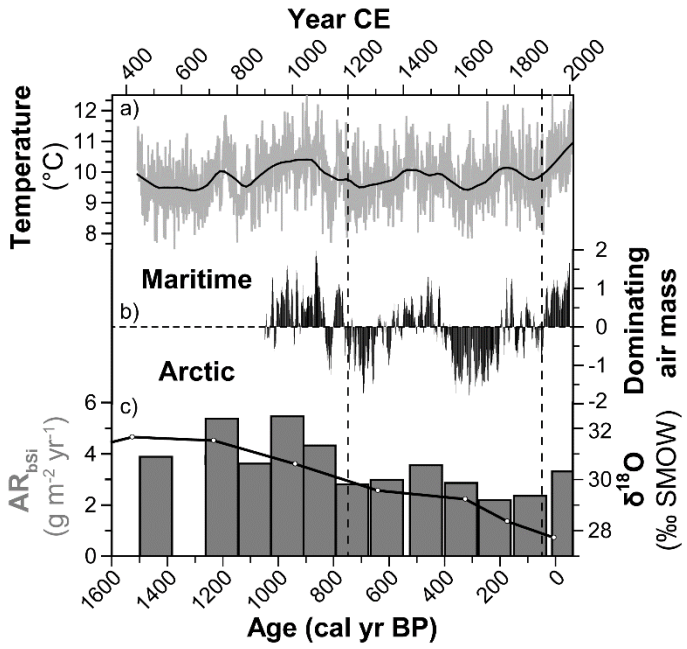

Figure 9. a) Summer (May to August) temperature reconstructions for the Torneträsk area based tree ring maximum late-wood-density (Melvin et al., 2012) and b) dominant atmospheric circulation based on departures between tree ring inferred temperature (X-ray density) and sunshine (stable carbon isotope ratio), where negative values indicate a dominance of cold-sunny weather (Arctic air dominant) and positive values indicate a dominance of warm-cloudy conditions (maritime air dominant) (Loader et al., 2013), compared to c) biogenic silica

742 accumulation rates (AR_{bSi}) and diatom-$\delta^{18}O$ of core Co1282 from Torneträsk for the period 1600
743 to -58 cal yr BP.

744

745 Ongoing environmental change following climate warming (1–0 cm blf; lithofacies D; 50 cal yr
746 BP to present)

747 During the past century, K and Al concentrations have returned to pre-LIA values, and K/Al
748 ratios and CI started to decline (Fig. 6). Together with the accompanying decline of C/N ratios
749 and $\delta^{15}N$, which both indicate a reduced soil-derived OM input to the lake, these data suggest a
750 stabilization of the catchment that has reduced soil erosion and terrestrial carbon export in the
751 Torneträsk area. This return to a sediment composition more similar to pre-750 cal yr BP can
752 only be linked to ongoing climate warming in the area, with a mean annual air temperature
753 increase of 2.5°C during the last century, that is also reflected in the recent increase in diatom
754 production (Figs. 8 and 9). Increased soil stabilization is corroborated by vegetation studies from
755 the Abisko area showing increases in vegetation growth rates and distributional range during the
756 past century (Callaghan et al., 2013, and references therein).

757 It is difficult to interpret the recent return to sedimentation in the western basin similar to that
758 prior to ~750 cal yr BP strictly from a climate perspective because of the increased human impact
759 in the area during the past centuries, including infrastructure development, increased reindeer
760 husbandry and more recently tourism. However, were these important, major environmental
761 disturbances such as the railroad (built AD 1898-1902) and highway (built AD 1980-1984)
762 construction along the southern shore of the lake would have caused opposite trends by
763 increasing soil disturbance and erosion, and have thus not led to discernable changes in the
764 sediment composition of Torneträsk's central western basin.

765

766 **5. Conclusions**

767 Although the dating of the sediment record from Torneträsk relies on a combination of directly
768 determined and inferred ages that we could transfer from a dated sediment record from a lake
769 located in one of Torneträsk's main subcatchments, the sediment record of this 330 km^2 lake
770 provides valuable insights into regional landscape-scale changes over the past c. 9500 yr. The
771 initial landscape development and accompanying lake ontogeny were the dominating influences
772 on sediment composition in Torneträsk after deglaciation. During the early to mid-Holocene,
773 gradual processes associated with the development of soils and vegetation drove the element
774 cycling in the aquatic and terrestrial environment and led to an initial nutrient (Si) limitation in
775 Torneträsk preventing notable diatom production until ~6600 cal yr BP. With progressing
776 ecosystem stabilization, the lake became more climate-sensitive during the late Holocene when
777 diatom production responded to climate variations (tree-ring inferred temperature) during the last
778 millennia, and a drop in diatom $\delta^{18}O$ suggests a larger shift in atmospheric circulation and/or
779 precipitation patterns.

780 In contrast to the successive change in the sediment composition following landscape
781 development, climate cooling during the late Holocene led to a pronounced shift in Torneträsk's
782 sediment composition that occurred rather abruptly (~100 years) but not before the onset of the
783 LIA around ~750 cal yr BP. This shift marking increased soil erosion was delayed by >2000
784 years compared to the first indications (tree-line retreat, increased erosion) for climate cooling
785 that are recorded in small lakes located in the Torneträsk catchment. The rather abrupt and
786 delayed compositional change in Torneträsk suggests a non-linear threshold response to climate
787 forcing. Following further climate cooling during the LIA, larger parts of the Torneträsk

watershed became susceptible to soil erosion, and from ~750 cal yr BP onwards environmental changes initially only registered in higher located sub-catchments more sensitive to tree-line dynamics were also registered in Torneträsk.

The second more rapid ecosystem change recorded in the sediment record of Torneträsk is related to the ongoing climate change that thus far has led to a return to pre-LIA conditions, which suggests catchment stabilization related to increased vegetation cover. In comparison to the previously recorded signals – gradual response to landscape development and abrupt but lagged response to climate cooling during the late Holocene, the lake ecosystem response to ongoing climate change is rather immediate, emphasizing the unprecedented scale of climate change in subarctic Fennoscandia during the past century.

Acknowledgements

We thank Florian Boxberg, Gerard Rocher Ros, Cristian Gudasz and Rolf Zale for their help in recovering sediment from Torneträsk and Abiskojaure. We also thank Peter Rosén, Thomas Westin and the Climate Impacts Research Centre (CIRC) in Abisko for their support as well as the Swedish Research Council and the "Stiftelsen J C Kempes Stipendiefond" for financial support. Fieldwork was supported by the EU INTERACT transnational access program. Hilary Sloane at the British Geological Survey undertook the O and Si isotope analysis of the diatom silica. We also thank the anonymous reviewers for their helpful comments and suggestions.

807 **References**

808 Adrian, R., O'Reilly, C.M., Zagarese, H., Baines, S.B., Hessen, D.O., Keller, W., Livingstone,
809 D.M., Sommaruga, R., Straile, D., Van Donk, E., Weyhenmeyer, G.A., Winder, M., 2009. Lakes
810 as sentinels of climate change. Limnol. Oceanogr. 54, 2283-2297.
811 Åkerman, H.J., Johansson, M., 2008. Thawing permafrost and thicker active layers in sub-arctic
812 Sweden. Permafrost and Periglacial Processes 19, 279-292.
813 Anderson, S.P., Drever, J.I., Frost, C.D., Holden, P., 2000. Chemical weathering in the foreland
814 of a retreating glacier. Geochim. Cosmochim. Acta 64, 1173-1189.
815 Andrén, H., Jonasson, C., Ottosson, J., 2002. Deltas in the Abisko area, northern Sweden: the
816 Abiskojokka delta in lake Torneträsk. Geogr. Ann. Ser. A-Phys. Geogr. 84A, 151-156.
817 Appleby, P., 2001. Chronostratigraphic techniques in recent sediments, In: Last, W.M., Smol,
818 J.P. (Eds.), Tracking environmental change using lake sediments. Vol. 1: Basin analysis, coring,
819 and chronological techniques. Kluwer Academic Publishers, Dordrecht, pp. 171-203.
820 Barnekow, L., 1999. Holocene tree-line dynamics and inferred climatic changes in the Abisko
821 area, northern Sweden, based on macrofossil and pollen records. Holocene 9, 253-265.
822 Barnekow, L., 2000. Holocene regional and local vegetation history and lake-level changes in the
823 Torneträsk area, northern Sweden. J. Paleolimn. 23, 399-420.
824 Barnekow, L., Possnert, G., Sandgren, P., 1998. AMS C-14 chronologies of Holocene lake
825 sediments in the Abisko area, northern Sweden - a comparison between dated bulk sediment and
826 macrofossil samples. GFF 120, 59-67.
827 Barnekow, L., Sandgren, P., 2001. Palaeoclimate and tree-line changes during the Holocene
828 based on pollen and plant macrofossil records from six lakes at different altitudes in northern
829 Sweden. Rev. Palaeobot. Palynology 117, 109-118.

Barnett, C., Dumayne-Peaty, L., Matthews, J.A., 2001. Holocene climatic change and tree-line response in Leirdalen, central Jotunheimen, south central Norway. Rev. Palaeobot. Palynology 117, 119-137.

Battarbee, R.W., Jones, V.J., Flower, R.J., Cameron, N.G., Bennion, H., Carvalho, L., Juggins, S., 2001. Diatoms. Springer, Netherlands.

Berger, A., Loutre, M. F., 1991. Insolation values for the climate of the last 10 million years, Quaternary Sci. Rev., 10, 297–317.

Berglund, B.E., Barnekow, L., Hammarlund, D., Sandgren, P., Snowball, I.F., 1996. Holocene forest dynamics and climate changes in the Abisko area, northern Sweden: the Sonesson model of vegetation history reconsidered and confirmed. Ecological Bulletins, 15-30.

Beylich, A.A., Sandberg, O., Molau, U., Wache, S., 2006. Intensity and spatio-temporal variability of fluvial sediment transfers in an Arctic-oceanic periglacial environment in northernmost Swedish Lapland (Latnjavagge catchment). Geomorphology 80, 114-130.

Bigler, C., Barnekow, L., Heinrichs, M.L., Hall, R.I., 2006. Holocene environmental history of Lake Vuolep Njakajaure (Abisko National Park, Northern Sweden) reconstructed using biological proxy indicators. Veg. Hist. Archaeobot. 15, 309-320.

Bigler, C., Grahn, E., Larocque, I., Jeziorski, A., Hall, R., 2003. Holocene environmental change at Lake Njulla (999 m asl), northern Sweden: a comparison with four small nearby lakes along an altitudinal gradient. J. Paleolimn. 29, 13-29.

Bigler, C., Larocque, I., Peglar, S.M., Birks, H.J.B., Hall, R.I., 2002. Quantitative multiproxy assessment of long-term patterns of Holocene environmental change from a small lake near Abisko, northern Sweden. Holocene 12, 481-496.

Blaauw, M., Christen, J.A., 2011. Flexible Paleoclimate Age-Depth Models Using an Autoregressive Gamma Process. Bayesian Anal. 6, 457-474.

854 Boyle, J.F., 2001. Inorganic geochemical methods in palaeolimnology, In: Last, W.M., Smol, J.P.
855 (Eds.), Tracking environmental change using lake sediments. Vol. 2: Physical and geochemical
856 methods. Kluwer Academic Publishers, Dordrecht, pp. 83-141.
857 Callaghan, T.V., Jonasson, C., Thierfelder, T., Yang, Z.L., Hedenås, H., Johansson, M., Molau,
858 U., Van Bogaert, R., Michelsen, A., Olofsson, J., Gwynn-Jones, D., Bokhorst, S., Phoenix, G.,
859 Bjerke, J.W., Tømmervik, H., Christensen, T.R., Hanna, E., Koller, E.K., Sloan, V.L., 2013.
860 Ecosystem change and stability over multiple decades in the Swedish subarctic: complex
861 processes and multiple drivers. Philos. Trans. R. Soc. B-Biol. Sci. 368.
862 Carrivick, J.L., Tweed, F.S., 2013. Proglacial lakes: character, behaviour and geological
863 importance. Quat. Sci. Rev. 78, 34-52.
864 Christensen, T.R., Johansson, T., Olsrud, M., Ström, L., Lindroth, A., Mastepanov, M., Malmer,
865 N., Friborg, T., Crill, P., Callaghan, T.V., 2007. A catchment-scale carbon and greenhouse gas
866 budget of a subarctic landscape. Philos. Trans. R. Soc. A-Math. Phys. Eng. Sci. 365, 1643-1656.
867 Dansgaard, W., 1964. Stable isotopes in precipetation. Tellus 16, 436-468.
868 Darmody, R.G., Thorn, C.E., Schlyter, P., Dixon, J.C., 2004. Relationship of vegetation
869 distribution to soil properties in Kärkevagge, Swedish Lapland. Arct. Antarct. Alp. Res. 36, 21-
870 32.
871 Elmendorf, S.C., Henry, G.H.R., Hollister, R.D., Bjork, R.G., Boulanger-Lapointe, N., Cooper,
872 E.J., Cornelissen, J.H.C., Day, T.A., Dorrepaal, E., Elumeeva, T.G., Gill, M., Gould, W.A.,
873 Harte, J., Hik, D.S., Hofgaard, A., Johnson, D.R., Johnstone, J.F., Jonsdottir, I.S., Jorgenson,
874 J.C., Klanderud, K., Klein, J.A., Koh, S., Kudo, G., Lara, M., Levesque, E., Magnusson, B., May,
875 J.L., Mercado-Diaz, J.A., Michelsen, A., Molau, U., Myers-Smith, I.H., Oberbauer, S.F.,
876 Onipchenko, V.G., Rixen, C., Schmidt, N.M., Shaver, G.R., Spasojevic, M.J., Porhallsdottir,
877 P.E., Tolvanen, A., Troxler, T., Tweedie, C.E., Villareal, S., Wahren, C.H., Walker, X., Webber,

878 P.J., Welker, J.M., Wipf, S., 2012. Plot-scale evidence of tundra vegetation change and links to
879 recent summer warming. Nat. Clim. Change 2, 453-457.
880 Emanuelsson, U., 1987. Human influence on vegetation in the Torneträsk area during the last
881 three centuries. Ecol. Bull., 95-111.
882 Fabel, D., Stroeven, A.P., Harbor, J., Kleman, J., Elmore, D., Fink, D., 2002. Landscape
883 preservation under Fennoscandian ice sheets determined from in situ produced Be-10 and Al-26.
884 Earth Planet. Sci. Lett. 201, 397-406.
885 Fabel, D., Fink, D., Fredin, O., Harbor, J., Land, M., Stroeven, A.P., 2006. Exposure ages from
886 relict lateral moraines overridden by the Fennoscandian ice sheet. Quaternary Res. 65, 136-146.
887 Gretener, B., Strömquist, L., 1981. Fluvioglacial landforms and ice margin characteristics - An
888 example from the Torneträsk area in northern Sweden. Geogr. Ann. Ser. A-Phys. Geogr. 63, 161-
889 168.
890 Gälman, V., Rydberg, J., Bigler, C., 2009. Decadal diagenetic effects on d13C and d15N studied
891 in varved lake sediment. Limnol. Oceanogr 54, 917-924.
892 Hammarlund, D., 1993. A distinct delta-C-13 decline in organic lake sediments at the
893 Pleistocene-Holocene transition in southern Sweden. Boreas 22, 236-243.
894 Hammarlund, D., Aravena, R., Barnekow, L., Buchardt, B., Possnert, G., 1997. Multi-component
895 carbon isotope evidence of early Holocene environmental change and carbon-flow pathways
896 from a hard-water lake in northern Sweden. J. Paleolimn. 18, 219-233.
897 Hammarlund, D., Barnekow, L., Birks, H.J.B., Buchardt, B., Edwards, T.W.D., 2002. Holocene
898 changes in atmospheric circulation recorded in the oxygen-isotope stratigraphy of lacustrine
899 carbonates from northern Sweden. Holocene 12, 339-351.
900 Hammarlund, D., Velle, G., Wolfe, B.B., Edwards, T.W.D., Barnekow, L., Bergman, J.,
901 Holmgren, S., Lamme, S., Snowball, I., Wohlfarth, B., Possnert, G., 2004. Palaeolimnological

902 and sedimentary reponses to Holocene forest retreat in the Scandes Mountains, west-central
903 Sweden. Holocene 14, 862-876.
904 Hinzman, L.D., Bettez, N.D., Bolton, W.R., Chapin, F.S., Dyurgerov, M.B., Fastie, C.L.,
905 Griffith, B., Hollister, R.D., Hope, A., Huntington, H.P., Jensen, A.M., Jia, G.J., Jorgenson, T.,
906 Kane, D.L., Klein, D.R., Kofinas, G., Lynch, A.H., Lloyd, A.H., McGuire, A.D., Nelson, F.E.,
907 Oechel, W.C., Osterkamp, T.E., Racine, C.H., Romanovsky, V.E., Stone, R.S., Stow, D.A.,
908 Sturm, M., Tweedie, C.E., Vourlitis, G.L., Walker, M.D., Walker, D.A., Webber, P.J., Welker,
909 J.M., Winker, K., Yoshikawa, K., 2005. Evidence and implications of recent climate change in
910 northern Alaska and other arctic regions. Clim. Change 72, 251-298.
911 Humborg, C., Smedberg, E., Blomqvist, S., Mörth, C.M., Brink, J., Rahm, L., Danielsson, A.,
912 Sahlberg, J., 2004. Nutrient variations in boreal and subarctic Swedish rivers: Landscape control
913 of land-sea fluxes. Limnol. Oceanogr. 49, 1871-1883.
914 Högberg, P., 1997. Tansley review No 95 - N-15 natural abundance in soil-plant systems. New
915 Phytol. 137, 179-203.
916 Jonsson, C.E., Leng, M.J., Rosqvist, G.C., Seibert, J., Arrowsmith, C., 2009. Stable oxygen and
917 hydrogen isotopes in sub-Arctic lake waters from northern Sweden. J. Hydrol. 376, 143-151.
918 Jonsson, C.E., Rosqvist, G.C., Leng, M.J., Bigler, C., Bergman, J., Tillman, P.K., Sloane, H.J.,
919 2010. High-resolution diatom delta O-18 records, from the last 150 years, reflecting changes in
920 amount of winter precipitation in two sub-Arctic high-altitude lakes in the Swedish Scandes. J.
921 Quat. Sci. 25, 918-930.
922 Karlén, W., 1988. Scandinavian glacial and climatic fluctuations during the Holocene. Quat. Sci.
923 Rev. 7, 199-209.

924 Karlsson, J., Christensen, T.R., Crill, P., Förster, J., Hammarlund, D., Jackowicz-Korczynski, M.,
925 Kokfelt, U., Roehm, C., Rosén, P., 2010. Quantifying the relative importance of lake emissions in
926 the carbon budget of a subarctic catchment. J. Geophys. Res. 115, G03006.
927 Kauppila, T., Salonen, V.P., 1997. The effect of Holocene treeline fluctuations on the sediment
928 chemistry of Lake Kilpisjarvi, Finland. J. Paleolimn. 18, 145-163.
929 Kokfelt, U., Rosén, P., Schoning, K., Christensen, T.R., Förster, J., Karlsson, J., Reuss, N.,
930 Rundgren, M., Callaghan, T.V., Jonasson, C., Hammarlund, D., 2009. Ecosystem responses to
931 increased precipitation and permafrost decay in subarctic Sweden inferred from peat and lake
932 sediments. Glob. Change Biol. 15, 1652-1663.
933 Kokfelt, U., Reuss, N., Struyf, E., Sonesson, M., Rudgren, M., Skog, G., Rosén, P., Hammarlund,
934 D., 2010. Wetland development, permafrost history and nutrient cycling inferred from late
935 Holocene peat and lake sediment records in subarctic Sweden. J. Paleolimn. 44, 327-342.
936 Krammer, K., Lange-Bertalot, H., 1986-91. Bacillariophyceae 1-4 Teil, In: Ettl, H., Gerloff, J.,
937 Heynig, H., Mollenhauer, D. (Eds.), Süsswasserflora von Mitteleuropa. Gustav Fischer Verlag,
938 Stuttgart/New York.
939 Kylander, M.E., Klaminder, J., Wohlfarth, B., Löwemark, L., 2013. Geochemical reponses of
940 paleoclimatic chnages in southern Sweden since the late glacial: the Hässeldala Port lake
941 sediment record. J. Paleolimn. 50, 57-70.
942 Law, K.R., Nesbitt, H.W., Longstaffe, F.J., 1991. Weathering of granitic tills and the genesis of a
943 podzol. Am. J. Sci. 291, 940-976.
944 Leng, M.J., Swann, G.E.A., Hodson, M.J., Tyler, J.J., Patwardhan, S.V., Sloane, H.J., 2009. The
945 Potential use of Silicon Isotope Composition of Biogenic Silica as a Proxy for Environmental
946 Change. Silicon 1, 65-77.

947 Loader, N.J., Young, G.H.F., Grudd, H., McCarroll, D., 2013. Stable carbon isotopes from
948 Torneträsk, northern Sweden provide a millennial length reconstruction of summer sunshine and
949 its relationship to Arctic circulation. Quat. Sci. Rev. 62, 97-113.
950 Lotter, A.F., Bigler, C., 2000. Do diatoms in the Swiss Alps reflect the length of ice-cover?
951 Aquat. Sci. 62, 125-141.
952 Lowick, S. E., Buechi, M. W., Gaar, D., Graf, H. F., Preusser, F., 2015. Luminescence dating of
953 Middle Pleistocene proglacial deposits from northern Switzerland: methodological aspects and
954 stratigraphical conclusions. Boreas 44, 459-482.
955 Magnuson, J.J., Robertson, D.M., Benson, B.J., Wynne, R.H., Livingstone, D.M., Arai, T., Assel,
956 R.A., Barry, R.G., Card, V., Kuusisto, E., Granin, N.G., Prowse, T.D., Stewart, K.M., Vuglinski,
957 V.S., 2000. Historical trends in lake and river ice cover in the Northern Hemisphere. Science 289,
958 1743-1746.
959 Makarov, M.I., Malysheva, T.I., Cornelissen, J.H.C., van Logtestijn, R.S.P., Glasser, B., 2008.
960 Consistent patterns of N-15 distribution through soil profiles in diverse alpine and tundra
961 ecosystems. Soil Biol. Biochem. 40, 1082-1089.
962 Malmer, N., Johansson, T., Olsrud, M., Christensen, T.R., 2005. Vegetation, climatic changes
963 and net carbon sequestration in a North-Scandinavian subarctic mire over 30 years. Glob. Change
964 Biol. 11, 1895-1909.
965 Matskovsky, V.V., Helama, S. 2014. Testing long-term temperature reconstruction based on
966 maximum density chronologies obtained by reanalysis of tree-ring data sets from northenmost
967 Sweden and Finland. Clim. Past 10(4),1473–1487.
968 Melander, O., 1977. Geomorphological map 30H Riksgränsen (east), 30I Abisko, 31H Reurivare
969 och 31I Vadvetjåkka. Description and assessment of areas of geomorphological importance.
970 Stockholms Universitet, Naturgeografiska Institutionen, Stockholm, Sweden.

971 Melvin, T., Grudd, H., Briffa, K.R., 2012. Potential bias in 'updating' tree-ring chronologies
972 using regional curve standardisation: re-processing 1500 years of Torneträsk density and ring-
973 width data. The Holocene 23(3), 364-373.
974 Meyer-Jacob, C., Vogel, H., Boxberg, F., Rosén, P., Weber, M., Bindler, R., 2014a. Independent
975 measurement of biogenic silica in sediments by FTIR spectroscopy and PLS regression. J.
976 Paleolimn. 52, 245-255.
977 Meyer-Jacob, C., Vogel, H., Gebhardt, A.C., Wennrich, V., Melles, M., Rosén, P., 2014b.
978 Biogeochemical variability during the past 3.6 million years recorded by FTIR spectroscopy in
979 the sediment record of Lake El'gygytgyn, Far East Russian Arctic. Clim. Past 10, 209-220.
980 Meyers, P.A., 2003. Applications of organic geochemistry to paleolimnological reconstructions:
981 a summary of examples from the Laurentian Great Lakes. Org. Geochem. 34, 261-289.
982 Meyers, P.A., Ishiwatari, R., 1993. Lacustrine organic geochemistry--an overview of indicators
983 of organic matter sources and diagenesis in lake sediments. Org. Geochem. 20, 867-900.
984 Morley, D.W., Leng, M.J., Mackay, A.W., Sloane, H.J., Rioual, P., Battarbee, R.W., 2004.
985 Cleaning of lake sediment samples for diatom oxygen isotope analysis. J. Paleolimn. 31, 391-
986 401.
987 Moulton, K.L., West, A.J., Berner, R.A., 2000. Solute flux and mineral mass balance approaches
988 to the quantification of plant effects on silicate weathering. Am. J. Sci. 300, 539-570.
989 Nesje, A., 2009. Latest Pleistocene and Holocene alpine glacier fluctuations in Scandinavia.
990 Quat. Sci. Rev. 28, 2119-2136.
991 Och, L.M., Müller, B., Voegelin, A., Ulrich, A., Göttlicher, J., Steiniger, R., Mangold, S.,
992 Vologina, E.G., Sturm, M., 2012. New insights into the formation and burial of Fe/Mn
993 accumulations in Lake Baikal sediments. Chem. Geol. 330, 244-259.

994 Opfergelt, S., Delmelle, P., 2012. Silicon isotopes and continental weathering processes:
995 Assessing controls on Si transfer to the ocean. C. R. Geosci. 344, 723-738.
996 Parker, A., 1970. An index of weathering for silicate rocks. Geol. Mag. 107, 501-504.
997 Pearson, R.G., Phillips, S.J., Loranty, M.M., Beck, P.S.A., Damoulas, T., Knight, S.J., Goetz,
998 S.J., 2013. Shifts in Arctic vegetation and associated feedbacks under climate change. Nat. Clim.
999 Change 3, 673-677.
1000 Peinerud, E.K., Ingri, J., Pontér, C., 2001. Non-detrital Si concentrations as an estimate of diatom
1001 concentrations in lake sediments and suspended material. Chem. Geol. 177, 229-239.
1002 Qiu, L., Williams, D.F., Gvorzdkov, A., Karabanov, E., Shimaraeva, M., 1993. Biogenic silica
1003 accumulation and paleoproductivity in the northern basin of Lake Baikal during the Holocene.
1004 Geology 21, 25.
1005 Reimer, P.J., Bard, E., Bayliss, A., Beck, J.W., Blackwell, P.G., Ramsey, C.B., Buck, C.E.,
1006 Cheng, H., Edwards, R.L., Friedrich, M., Grootes, P.M., Guilderson, T.P., Haflidason, H.,
1007 Hajdas, I., Hatté, C., Heaton, T.J., Hoffmann, D.L., Hogg, A.G., Hughen, K.A., Kaiser, K.F.,
1008 Kromer, B., Manning, S.W., Niu, M., Reimer, R.W., Richards, D.A., Scott, E.M., Southon, J.R.,
1009 Staff, R.A., Turney, C.S.M., van der Plicht, J., 2013. IntCal13 and marine13 radiocarbon age
1010 calibration curves 0-50,000 years cal BP. Radiocarbon 55, 1869-1887.
1011 Reynolds, R.L., Rosenbaum, J.G., Rapp, J., Kerwin, M.W., Bradbury, J.P., Colman, S., Adam,
1012 D., 2004. Record of late Pleistocene glaciation and deglaciation in the southern Cascade Range. I.
1013 Petrological evidence from lacustrine sediment in Upper Klamath Lake, southern Oregon. J.
1014 Paleolimn. 31, 217-233.
1015 Rosén, P., Vogel, H., Cunningham, L., Hahn, A., Hausmann, S., Pienitz, R., Zolitschka, B.,
1016 Wagner, B., Persson, P., 2011. Universally applicable model for the quantitative determination of

1017 lake sediment composition using Fourier transform infrared spectroscopy. Environ. Sci. Technol.
1018 45, 8858–8865.
1019 Rosqvist, G., Jonsson, C., Yam, R., Karlén, W., Shemesh, A., 2004. Diatom oxygen isotopes in
1020 pro-glacial lake sediments from northern Sweden: a 5000 year record of atmospheric circulation.
1021 Quat. Sci. Rev. 23, 851-859.
1022 Rosqvist, G.C., Leng, M.J., Goslar, T., Sloane, H.J., Bigler, C., Cunningham, L., Dadal, A.,
1023 Bergman, J., Berntsson, A., Jonsson, C., Wastegård, S., 2013. Shifts in precipitation during the
1024 last millennium in northern Scandinavia from lacustrine isotope records. Quat. Sci. Rev. 66, 22-
1025 34.
1026 Rosqvist, G.C., Leng, M.J., Jonsson, C., 2007. North Atlantic region atmospheric circulation
1027 dynamics inferred from a late-Holocene lacustrine carbonate isotope record, northern Swedish
1028 Lapland. Holocene 17, 867-873.
1029 Roy, P.D., Caballero, M., Lozano, R., Smykatz-Kloss, W., 2008. Geochemistry of late quaternary
1030 sediments from Tecocomulco lake, central Mexico: Implication to chemical weathering and
1031 provenance. Chem. Erde 68, 383-393.
1032 Rühland, K.M., Paterson, A.M., Smol, J.P., 2015. Lake diatom response to warming: reviewing
1033 the evidence. J. Paleolimn. 54, 1-35.
1034 Rubensdotter, L., Rosqvist, G., 2003. The effect of geomorphological setting on Holocene lake
1035 sediment variability, northern Swedish Lapland. J. Quat. Sci. 18, 757-767.
1036 Rydberg, J., Klaminder, J., Rosén, P., Bindler, R., 2010. Climate driven release of carbon and
1037 mercury from permafrost mires increases mercury loading to sub-arctic lakes. Sci. Total Environ.
1038 408, 4778-4783.

1039 Rydberg, J., 2014. Wavelength dispersive X-ray fluorescence spectroscopy as a fast, non-
1040 destructive and cost-effective analytical method for determining the geochemical composition of
1041 small loose-powder sediment samples. J. Paleolimn. 52, 265-276.
1042 Schuur, E.A.G., McGuire, A.D., Schadel, C., Grosse, G., Harden, J.W., Hayes, D.J., Hugelius,
1043 G., Koven, C.D., Kuhry, P., Lawrence, D.M., Natali, S.M., Olefeldt, D., Romanovsky, V.E.,
1044 Schaefer, K., Turetsky, M.R., Treat, C.C., Vonk, J.E., 2015. Climate change and the permafrost
1045 carbon feedback. Nature 520, 171-179.
1046 Seppä, H., Birks, H.J.B., 2001. July mean temperature and annual precipitation trends during the
1047 Holocene in the Fennoscandian tree-line area: pollen-based climate reconstructions. Holocene 11,
1048 527-539.
1049 Seppä, H., Bjune, A.E., Telford, R.J., Birks, H.J.B., Veski, S., 2009. Last nine-thousand years of
1050 temperature variability in Northern Europe. Clim. Past. 5, 523-535.
1051 Shemesh, A., Rosqvist, G., Rietti-Shati, M., Rubensdotter, L., Bigler, C., Yam, R., Karlén, W.,
1052 2001. Holocene climatic change in Swedish Lapland inferred from an oxygen-isotope record of
1053 lacustrine biogenic silica. Holocene 11, 447-454.
1054 Snowball, I., Sandgren, P., 1996. Lake sediment studies of Holocene glacial activity in the Karsa
1055 valley, northern Sweden: Contrasts in interpretation. Holocene 6, 367-372.
1056 Stevenson, A.C., Juggins, S., Birks, H.J.B., Anderson, D.S., Anderson, N.J., Battarbee, R.W.,
1057 Berge, F., Davis, R.B., Flower, R.J., Haworth, E.Y., Jones, V.J., Kingston, J.C., Kreiser, A.M.,
1058 Line, J.M., Munro, M.A.R., Renberg, I., 1991. The surface waters acidification programme:
1059 Modern diatom/lake-water chemistry data-sets. ENSIS Publishing, London.
1060 Stroeven, A.P., Fabel, D., Harbor, J., Hättestrand, C., Kleman, J., 2002. Quantifying the erosional
1061 impact of the Fennoscandian ice sheet in the Tornetrask-Narvik corridor, northern Sweden, based
1062 on cosmogenic radionuclide data. Geogr. Ann. Ser. A-Phys. Geogr. 84A, 275-287.

Swann, G.E.A., Leng, M.J., Juschus, O., Melles, M., Brigham-Grette, J., Sloane, H.J., 2010. A combined oxygen and silicon diatom isotope record of Late Quaternary change in Lake El'gygytgyn, North East Siberia. Quat. Sci. Rev. 29, 774-786.

Vogel, H., Rosén, P., Wagner, B., Melles, M., Persson, P., 2008. Fourier transform infrared spectroscopy, a new cost-effective tool for quantitative analysis of biogeochemical properties in long sediment records. J Paleolimn. 40, 689-702.

Vogel, H., Wagner, B., Rosén, P., 2013. Lake Floor Morphology and Sediment Architecture of Lake Tornetrask, Northern Sweden. Geogr. Ann. Ser. A-Phys. Geogr. 95A, 159-170.

Vonk, J.E., Alling, V., Rahm, L., Morth, C.M., Humborg, C., Gustafsson, O., 2012. A centennial record of fluvial organic matter input from the discontinuous permafrost catchment of Lake Torneträsk. J. Geophys. Res. 117, G03018.

Whitehead, D.R., Charles, D.F., Jackson, S.T., Smol, J.P., Engstrom, D.R., 1989. The developmental history of Adirondack (NY) lakes. J. Paleolimn. 2, 185-206.

Williamson, C.E., Saros, J.E., Vincent, W.F., Smol, J.P., 2009. Lakes and reservoirs as sentinels, integrators, and regulators of climate change. Limnol. Oceanogr. 54, 2273-2282.

Wolfe, B.B., Edwards, T.W.D., Aravena, R., 1999. Changes in carbon and nitrogen cycling during tree-line retreat recorded in the isotopic content of lacustrine organic matter, western Taimyr Peninsula, Russia. Holocene 9, 215-222.

Xu, L., Myneni, R.B., Chapin, F.S., Callaghan, T.V., Pinzon, J.E., Tucker, C.J., Zhu, Z., Bi, J., Ciais, P., Tommervik, H., Euskirchen, E.S., Forbes, B.C., Piao, S.L., Anderson, B.T., Ganguly, S., Nemani, R.R., Goetz, S.J., Beck, P.S.A., Bunn, A.G., Cao, C., Stroeve, J.C., 2013. Temperature and vegetation seasonality diminishment over northern lands. Nat. Clim. Change 3, 581-586.

1086 Zhang, W., Miller, P.A., Smith, B., Wania, R., Koenigk, T., Döscher, R., 2013. Tundra
1087 shrubification and tree-line advance amplify arctic climate warming: results from an individual-
1088 based dynamic vegetation model. Environ. Res. Lett. 8, 034023.